Scarless whole-body regeneration in the absence of a blastema requires cell division in the ctenophore *Mnemiopsis leidyi*

Authors:

Julia Ramon Mateu[1], Mark Q. Martindale[1*]

Affiliation:

[1]The Whitney Laboratory for Marine Bioscience, 9505 N, Ocean Shore Blvd, St. Augustine, FL 32080-8610, USA

*Corresponding author

Email: mqmartin@whitney.ufl.edu

ABSTRACT

It has been known for well over 50 years that ctenophores have the capacity to regenerate but the cellular and molecular mechanisms underlying this ability are unknown. We have studied wound healing and adult regeneration in the ctenophore *Mnemiopsis leidyi* and show that cell proliferation is activated at the wound site and is indispensable for whole-body regeneration. Wound healing occurs normally in the absence of cell proliferation forming a scar-less wound epithelium. No blastema is generated, rather undifferentiated cells assume the correct location of missing structures and differentiate in place. Proliferative cells from the uncut tissue migrate to the wound site and contribute to the formation of new structures. Surprisingly, the ability to regenerate is recovered when exposure to cell-proliferation blocking treatment ends, suggesting that the onset of regeneration is constantly ready to be triggered and it is somehow independent of the wound healing process.

INTRODUCTION

Regeneration, the ability to re-form a body part that has been lost, is a widely shared property among metazoans (Bely and Nyberg, 2010). However, the contribution of cell proliferation and the source of regenerating tissue varies greatly among animals with regenerative ability, resulting in a collection of different modes of regenerative (Alvarado and Tsonis, 2006; Tanaka and Reddien, 2011). The first classification of regenerative strategies was established by T. H. Morgan who initially defined two different mechanisms of rebuilding structures according to the contribution of cell proliferation: 1) *morphallaxis*, regeneration which occurs in the absence of active cell proliferation, through re-patterning of pre-existing tissue, and 2) *epimorphosis*, regeneration mediated by cell proliferation (Morgan, 1901). Epimorphic regeneration can involve the production of a blastema, a mass of undifferenciated cells that forms at the wound site from where cells proliferate and differentiate to form the missing structures (Sánchez Alvarado, 2000). The classical example of morphallactic regeneration is provided by the freshwater cnidarian polyp *Hydra*, which is able to regenerate both head and foot without a significant contribution from cell proliferation (Park et al., 1970; Cummings and Bode, 1984; Dübel and Schaller, 1990; Holstein et al., 1991). While documented cases of strict morphallaxis are very few in nature, most of the organisms with regenerative potential rely on cell proliferation (epimorphosis) – or a combination of both epimorphosis and morphallaxis – to re-form lost structures. Regenerative abilities appear to be diverse even within individual evolutionary clades. For example, regeneration of oral structures in another member of the phylum Cnidaria – *Nematostella vectensis* – is characterized by high levels of cell proliferation differing thus from the morphallactic regeneration potential in *Hydra* (Passamaneck and Martindale, 2012). In planarians, whole-body regeneration is accomplished by the proliferation of pluripotent stem cells (called neoblasts), the only cells in the animal that are capable of cell proliferation, which form a mass of undifferentiated cells known as the regenerating blastema (Baguna et al., 1989; Newmark and Sánchez Alvarado, 2000; Wagner et al., 2011). Annelid regeneration provides examples of both epimorphic (blastema-based) regeneration and morphallactic (tissue-remodeling based) regeneration (Bely, 2014; Özpolat and Bely, 2016), showing diversity within the Lophotrochozoa. Moreover, evidence of cell migration has been documented during regeneration of several annelid species such as the freshwater annelid *Pristina leidyi* (Zattara et al., 2016) or the marine annelid worm *Capitella teleta,* in which local (proliferating cells close to the wound site) and distant (stem cell migration) sources of cells contribute to the formation of the regenerating blastema (de Jong and Seaver, 2017). Evidence of cell migration during regeneration is also provided by the hydrozoan *Hydractinia echinata* in which stem cells (i-cells) from a

remote area migrate to the wound site and contribute in the formation of the blastema (Bradshaw et al., 2015). In vertebrates, the potential of regeneration is limited to the structural or cellular level. Urodele amphibians are known for being the only vertebrate tetrapods that can regenerate amputated limbs as adults. Similarly to the previous examples of epimorphic regeneration, they require cell proliferation and the formation of a blastema, however, the urodele blastema is not generated from or composed of cells of a single type, but it consists in a heterogeneous collection of lineage-restricted progenitors (Kragl et al., 2009).

Among the animals with regenerative capabilities are lobate ctenophores (comb jellies), fragile holopelagic marine carnivores that represent one of the oldest extant metazoan lineages. Ctenophora is latin for “comb bearer”, referring to eight longitudinally oriented rows of locomotory ctene (or comb) plates which they coordinately beat to propel through the water column. Ctenphores possess a highly unique body plan characterized by a biradial symmetry (with no planes of mirror symmetry) and two epithelial layers: the ectoderm and the endoderm, separated by a thick mesoglea mostly composed of extracellular matrix, but also containing several types of individual muscle and mesenchymal cells. The oral-aboral axis is their major body axis and it is characterized by the mouth at one (oral) pole and the apical sensory organ at the opposite (aboral) pole. Most ctenophores possess a pair of muscular tentacles that bear specialized adhesive cells called colloblasts, used to capture prey (Pang and Martindale, 2008). One of the best studied species of ctenophores is the lobate ctenophore *Mnemiopsis leidyi,* which is emerging as a new model system in evolutionary-developmental biology (Henry and Martindale, 2000; Fischer et al., 2014; Schnitzler et al., 2014; Jager and Manuel, 2016; Reitzel et al., 2016; Martindale, 2016). *M. leidyi*’s life cycle is characterized by a rapid development including a highly stereotyped cleavage program and two adult stages: the juvenile tentaculate cydippid, distinguishable for having a pair of long branching tentacles, and the lobate adult form which possess two oral feeding lobes. A particular feature of ctenophore embryogenesis is that they undergo mosaic development, meaning that embryos cannot compensate for cells/structures derived from cells killed or isolated during early development. If blastomeres are separated at the two-cell stage, each will generate a “half-animal,” possessing exactly half of the normal set of adult features (Freeman, 1967; Martindale, 1986). This lack of ability to replace missing parts during embryogenesis contrasts with the outstanding capacity to regenerate as adults. Both the tentaculate larval and lobate adult life stages of *M. leidyi* readily regenerate and are capable of whole-body regeneration from only a body quadrant or half (Martindale, 1986).

It has been known for well over 50 years that ctenophores have the capacity to replace missing body parts (Coonfield, 1936; Martindale, 1986; Martindale and Henry, 1996; Henry and Martindale, 2000; Tamm, 2012) but the cellular and molecular mechanisms underlying this ability are poorly understood. Is cell proliferation required for ctenophore regeneration? Is any kind of blastema-like structure formed during regeneration? Does scarring occur during the wound healing process? What is the source and nature of cells that contribute to the regenerated structures? What is the role of the wound epidermis in regulating the future regenerative outcome? We have studied wound healing and adult regeneration in the ctenophore *Mnemiopsis leidyi* and show that cell proliferation is activated at the wound site and it is indispensable for the regeneration of all the structures of the cydippid's body. Wound healing occurs normally in the absence of cell proliferation forming a scar-less wound epithelium only a few hours after amputation. In both animals cut in half and those in which the apical organ is removed, anlage of all missing structures occurs within 48 hours and complete replacement of all cell types by 72 hours after the injury. No blastema is generated, rather undifferentiated cells assume the correct location of missing structures and differentiate in place. EdU (5-ethynyl-2'-deoxyuridine) labeling shows that in uncut animals the majority of cell divisions occur in the tentacle bulbs where the tentacles are continuously growing. In surgically challenged animals, cell division is stimulated 6 hours after cutting both at the cut site as well as throughout the rest of the body and continues until 48 hours. The appearance of new structures is completely dependent on cell division, however, surprisingly, the ability to regenerate is recovered when exposure to cell-proliferation blocking treatment ends, suggesting that the onset of regeneration is constantly ready to be triggered and it is somehow independent of the wound healing process. This study provides some first-time insights of the cellular mechanisms involved in ctenophore regeneration and paves the way for future molecular studies that will contribute to the understanding of the evolution of regenerative ability throughout the animal kingdom.

MATERIALS AND METHODS

Animal care

Regeneration experiments were performed on juvenile *Mnemiopsis leidyi* cydippid stages due to their small size and ease of visualization and because their power of regeneration is the same as adults. *M. leidyi* cydippids were obtained from spawning adults collected from either the floating docks located around Flagler Beach area, FL. USA, or from the floating docks at the east end of the Bridge of Lions on Anastasia Island, St. Augustine, FL. USA. For spawning, freshly collected adults were kept in constant light

for at least two consecutive nights and then individual animals transferred into 6" diameter glass culture dishes filled with 1x FSW and placed in total darkness. After approximately 3-4 hours in the dark at 22-24ºC, these self-fertile hermaphroditic animals had spawned and embryos were collected by pipetting them into a new dish of UV treated 1.0 micron filtered full strength seawater (1x FSW) using a transfer pipette. Embryos were raised to the juvenile *cydippid* stage at 22-24ºC.

Animal surgeries

Cydippids were fed with rotifers (*Brachionus plicatilis*, 160µm) (Reed Mariculture, Inc) once a day until they were approximately 1.5-3.0 mm in diameter (approximately 5-7 days post spawning). Operations were done in 35 mm plastic petri dishes with 2 mm thick silicon-coated bottom (SYLGARD–184, Dow Corning, Inc.). Cydippids were transferred in to the operation dishes in 0.2µm-filtered seawater and cut using hand pulled glass needles from Pyrex capillaries (Martindale, 1986). Two types of operations were performed: 1) Oral-aboral bisections, in which animals were cut longitudinally through the esophageal plane generating two "half-animals". The operations were performed such that one half retained an intact apical organ while the remaining half lacked the apical organ. Only the halves retaining the apical organ were studied here as these halves regenerate to normal animals in a high percentage of the cases (Martindale, 1986). 2) Apical organ amputations, involving the removal of the apical organ by cutting perpendicular to the oral-aboral axis above the level of the tentacle bulbs. Following amputation, halves containing the apical organ and amputated cydippids without apical organ were returned to 35 mm plastic Petri dishes filled with 0.2µm filtered 1x FSW for the desired length of time. All the regenerating experiments were performed at 22-24ºC.

Tissue labeling and cell counts

Detection of cell proliferation by incorporation of EdU

To label proliferating cells, cydippids were fixed and processed for fluorescent detection of incorporated EdU using the Click-iT EdU labeling kit (Invitrogen, Carlsbad, CA, USA), which incorporates EdU in cells that are undergoing the S phase of the cell cycle. Specifically, intact cydippids between 1.5-3.0 mm in diameter or bisected/amputated cydippids were incubated in EdU labeling solution (100 µM of EdU in 1x FSW) for 15 minutes. For pulse-chase experiments cydippids were incubated with 100 µM EdU in 1x FSW for 15 minutes, washed 3 times with 100 µM thymidine in 1x FSW, and maintained in increasing volumes of 1x FSW until fixation. Control or operated cydippids were embedded in 1.2% low melt agarose (25ºC melting temperature, USB, Inc Cat #32830) in a 35 mm plastic petri dish (Fisher, Inc. Cat #08757100A) and fixed in ice-cold 100mM

HEPES pH 6.9; 0.05M EGTA; 5mM MgSO4; 200mM NaCl; 1x PBS; 3.7% Formaldehyde; 0.2% Glutaraldehyde; 0.2% Triton X-100; and 1x FSW (0.2 µm filtered) for 1 hour at room temperature in gentle rocking (Salinas-Saavedra and Martindale, 2018). Animals were then washed several times in PBS-0.02% Triton X-100, then one time in PBS-0.2% Triton X-100 for 20 min, and again several times in PBS-0.02% Triton X-100. The EdU detection reaction was performed according to manufacturer instructions using the Alexa-567 reaction kit. Following detection, cydippids were washed three times in PBS-0.02% Triton X-100, and subsequently all nuclei were counterstained with DAPI (Invitrogen, Inc. Cat. # D1306) at 0.1µg/µl in 1x PBS for 30 minutes. Cydippids were mounted in TDE mounting media (97% TDE: 970µl 2,2'-thiodiethanol (Sigma-Aldrich, Inc); 30µl PBS) for visualization. To quantify the percentage of EdU labeled cells at the wound site, Zeiss 710 confocal z-stack projections of operated and control cydippids were generated using Fiji software (Image J) and individual cells were digitally counted using Imaris, Inc. software (Bitplane, Switzerland). Only the the area and z-stacks corresponding to the wound site were used for the analysis. EdU+ cells and nuclei were counted separately in more than 3 specimens for each time-point. The number of EdU-positive nuclei were divided by the total number of nuclei generating a ratio corresponding to the % of EdU+ cells. Average values ± standard error were represented in linear graphs.

Immunofluorescence

Proliferating cells in M phase were detected using an antibody against phospho Histone 3 (PH3 – phospho S10). Control or operated cydippids were fixed as mentioned above. Fixed cydippids were washed several times in PBS-0.02% Triton X-100 (PBT 0.02%), then one time in PBS-0.2% Triton X-100 (PBT 0.2%) for 10 min, and again several times in PBT 0.02%. They were then blocked in 5% normal goat serum (NGS; diluted in PBT 0.2%) for 1 hour at room temperature with gentle rocking. After blocking, specimens were incubated in anti-phospho histone H3 antibody (ARG51679, arigobio) diluted 1:150 in 5% NGS overnight at 4ºC. The day after, specimens were washed at least five times with PBS-0.2% Triton X-100. Secondary antibody (Alexa Fluor 488 goat anti-rabbit IgG [A-11008, Invitrogen]) was diluted 1:250 in 5% NGS and incubated over night at 4ºC with gentle rocking. After incubation, specimens were washed three times with PBT 0.02% and incubated with DAPI (0.1µg/µl in 1x PBS; Invitrogen, Inc. Cat. # D1306) for 2 hours to allow nuclear visualization. Samples were then rinsed in 1x PBS and mounted in TDE mounting media (97% TDE: 970µl 2,2'-thiodiethanol (Sigma-Aldrich, Inc); 30µl PBS) for visualization.

Cell proliferation inhibitor treatment with Hydroxyurea (HU)

Cell proliferation was blocked using the ribonucleotide reductase inhibitor hydroxyurea (HU) (Sigma-Aldrich, St. Louis, MO, USA). Incubations with hydroxyurea were performed at a concentration of 5 mM in 1x FSW. Operated cydippids were exposed to continuous incubations of 5mM HU for 48-72 hours. HU solution was exchanged with freshly diluted inhibitor every 12 hours. For washing experiments, the effect of HU was reversed by removal and replacement of the drug with 1x FSW.

Imaging

In vivo differential interference contrast (DIC) images were captured using a Zeiss Axio Imager M2 coupled with an AxioCam (HRc) digital camera. Fluorescent confocal imaging was performed using a Zeiss LSM 710 confocal microscope (Zeiss, Gottingen, Germany) using either a 20x/0.8 NA dry objective or a 40x/1.3 NA oil immersion objective. Generation of Z-stack projections and image processing was performed using Fiji software (Image J).

RESULTS

Whole-body regeneration in *Mnemiopsis leidyi* cydippids

Although the regenerative response has been studied previously in *M. leidyi* (Coonfield, 1936; Martindale, 1986; Martindale and Henry, 1996; Henry and Martindale, 2000; Tamm, 2012) we first characterized the sequence of morphogenic events during cydippid regeneration to provide a baseline for further experimental investigations. For this, two types of surgeries – covering all the structures of the cydippid's body (apical organ, comb rows, tentacle bulbs and tentacles) – were performed (**Figure 1**). The timing and order of formation of missing structures was assessed by *in vivo* imaging of the regenerating animals at different time points along the regeneration process.

Events during whole-body regeneration of the M. leidyi cydippid following bisection through the oral-aboral axis

Cydippids were bisected through the oral-aboral axis retaining the whole apical organ in one of the halves – bisected cydippids with a complete intact apical organ regenerate into whole animals in a higher percentage of the cases compared to bisected animals with half apical organ (Martindale, 1986). Bisected cydippids containing half of the set of structures present in intact cydippids (four comb rows and one tentacle) and a complete apical organ were left to regenerate in 1x filtered sea water (1x FSW) (n>100) at 22ºC. Wound closure was initiated rapidly after bisection with the edges of the wound forming a round circumference that continued to reduce in diameter until meeting and was

completed within 2 hours after bisection (hab). No scar or trace of the original wound was evident after this time. About 16 hab, four ciliated furrows – which connect the apical organ with the comb rows – appeared on a surface epithelium at the aboral end of the cut site (**Figure 2B**). A large blastema or mass of undifferentiated cells did not appear at the cut site. Rather, accumulations of cells were detected forming the primordia of all four of the future comb rows in a deeper plane at the end of each ciliated furrow. By 24 hab, the first comb plates appeared, first in the two most external (closer to existing comb rows) comb rows and later in the two internal ones (**Figure 2C**). Comb plate formation did not follow a consistent pattern initially. The correct orientation of comp plates and coordination of their beating was accomplished after a number of comb plates were formed (**Figure 2D** surface, down), as has been described previously (Tamm, 2012). Within 40 hab, coordinated comb plates were beating in all four regenerating comb rows and the primordia of tentacle bulb had emerged in the middle of the four comb rows. By 48 hab, regeneration of the missing structures of the cydippid body was essentially completed including the formation of the tentacle growing from the tentacle bulb (**Figure 2E**). At 96 hours after bisection, the regenerated tentacle was long enough to actively catch pray. The cut side continued to grow and within a day or two was indistinguishable from the uncut side (**Figure 2F**).

Events during regeneration of the M. leidyi cydippid following apical organ amputation

Cydippids in which the apical organ was amputated (**Figure 1**) were left to regenerate in 1x FSW (n>100). The cut edges of the wound met and sealed over within 30-60 min of the operation and the lesion was completely healed around 2 hours post amputation (hpa). Between 6 and 12 hpa cells congregated under the wounded epithelium forming the primordia of the future apical organ (**Figure 3E-F'**). Extension of the ciliated furrows from each comb row towards the wound site could be spotted around 12 hpa. Within 24 hpa, cells at the wound site started to differentiate into the apical organ floor and supporting cilia (**Figure 3G-H'**). At 48 hpa all the components of the statolith, including the supporting cilia, the balancing cilia and lithocytes, were formed (**Figure 3I-J'**). At approximately 60 hpa the complete set of structures forming the apical organ were regenerated with the exception of the polar fields (Figure 3K-L'). Within 3 days after amputation animals had regenerated the entire apical organ structure and were indistinguishable from control animals of the same size.

Cell proliferation in intact cydippids

To identify the areas of cell proliferation in juvenile *M. leidyi*, intact cydippids between 1.5 – 3.0 mm in diameter were labelled with the thymidine analog 5-ethynyl-20-

deoxyuridine (EdU), which is incorporated into genomic DNA during the S-phase of the cell cycle (Salic and Mitchison, 2008; Chehrehasa et al., 2009; Alié et al., 2011; Schnitzler et al., 2014) (**Figure 4A**). Cydippids incubated with EdU during a 15-minute pulse showed a pattern of cell division characterized by two main regions of active cell proliferation corresponding to the tentacle bulbs. EdU labeling was also found in some cells of the apical organ and few isolated cells along the pharynx and under the comb rows (**Figure 4B-D'**). To detect dividing cells in M phase of the cell cycle we performed anti-phospho-histone 3 (anti-PH3) immunolabelings in intact cydippids. The spatial pattern and distribution of PH3 labeling closely matched the one described for EdU incorporation, although PH3+ cells were always about 10% less numerous than the EdU labeled cells, suggesting that the duration of the M phase is much shorter than S phase.

In order to track the populations of proliferating cells over time we performed EdU pulse-chase experiments consisting in a 15-minute EdU incubation (pulse) and a chase of different times followed by visualization (**Figure 4A**). After a 24h chase, the pools of proliferating cells had migrated from the tentacle bulb through the proximal region of the tentacles, although some EdU+ cells were still detected at the tentacle sheath. Increased labeling of nuclei in the apical organ, pharynx and comb rows was also observed (**Figure 4E-F'**), suggesting that cells migrated in to those regions from regions of high mitotic density. Following a 48h chase, the population of proliferating cells that was originally in the tentacle bulbs at the time of labeling had migrated to the most distal end of the tentacles, but some EdU+ nuclei remained in the tentacle bulbs, suggesting that there is a resident population of slowly dividing stem cells in the tentacle bulb. The number of EdU+ nuclei along the pharynx, the apical sensory organ (specifically in the apical organ floor) and comb rows was considerably increased compared to the 24h chase condition (**Figure 4G-G'**), suggesting that EdU labeled cells had proliferated during the chase period. To closely analyze the migration of proliferating cells along the tentacles we performed EdU pulse-chase experiments in smaller windows of time. Results show movement of EdU label from the tentacle sheath (t=0h) (**Figure 4H-H'**) to the most distal end of the tentacle (t=48h) (**Figure 4K-K'**) passing through the tentacle sheath (t=6h) (**Figure 4I-I'**) and proximal region of the tentacle (t=12h) (**Figure 4J-J'**).

Cell proliferation is activated during ctenophore regeneration

Regeneration can be classified into two general groups according to the involvement of cell proliferation: epimorphosis, in which regeneration is mediated by active cell proliferation, and morphallaxis, in which regeneration can occur in the absence of cell proliferation, due to the remodeling of pre-existing cells (Alejandro Sánchez, 2000). In order to determine the role of cell proliferation in ctenophore regeneration we performed

a series of EdU experiments in regenerating cydippids. 15-minute exposure to EdU at different times after surgical cutting was evaluated after two types of surgeries: a bisection through the oral-aboral axis and an apical organ ablation.

Following oral-aboral bisection, EdU+ cells were first detected at the wound site at 6 hab. The few EdU+ nuclei were scattered throughout the cut site without forming any evident pattern (**Figure 5C- C'**). The number of EdU labeled nuclei at the wound site slightly increased between 6 and 12 hab. At 12 hab proliferating cells were also scattered all along the cut site but no aggregation of cells was observed (**Figure 5D-E'**). At 24 hab the number of EdU+ cells had markedly increased and was concentrated in discrete areas forming the primordia of the regenerating tissues (the tentacle bulb and comb rows) (**Figure 5F-G'**). Between 24 and 48 hab proliferative cells were focalized at the oral end of the regenerating comb rows – which are formed in an aboral towards oral direction – and the regenerating tentacle bulb. Proliferative cells were no longer detected at the aboral end of the comb rows where cells had already differentiated into comb plates (**Figure 5I'**). By 96 hab, when major repatterning events of regeneration were completed, EdU+ cells were only detected at the regenerated tentacle sheath forming the pattern of cell proliferation previously described in the tentacle bulbs of intact cydippids (**Figure 4**) (**Supplementary Figure 1**).

EdU labeling was also detected in regenerating cydippids after apical organ amputation. To quantify cell proliferation, the ratio of EdU+ nuclei to total nuclei was calculated at different time-points following amputation (**Figure 6B**). EdU+ cells were first detected between 6 and 12 hpa. There was some variability in the presence of EdU+ nuclei at 6 hpa – with some specimens depleted of EdU+ nuclei at the wound site, however the presence of EdU+ cells was consistent in all the analyzed individuals at 12 hpa. (**Figure 6C-D''**). A peak of cell proliferation was observed at 24hpa, with EdU+ cells localized at the primordia of the apical organ, specifically in the apical organ floor, and in the surrounding tissue including the regenerating comb rows adjacent to the cut site (**Figure 6E-F''**). The number of proliferating cells slightly decreased at 48 hpa when EdU+ cells were concentrated in the regenerating apical organ and were no longer found in the tissues near the wound site (**Figure 6G-H''**). In combination with EdU incorporation experiments, anti-PH3 immunostaining was performed at selected time-points following amputation. PH3+ cells were detected in the regenerating structures of the apical organ at 24 hpa (**Figure 6I-I''**) and 48 hpa (**Supplementary Figure 2**) consistent with the EdU incorporation, although the number of PH3+ cells was always less numerous than the EdU+ cells.

Interestingly, for both types of surgeries, proliferating cells were not organized in a compacted mass of "blastema-like" cells from were new tissue formed. In contrast,

proliferating cells were very few and scattered throughout the wound site at early time-points after surgery – when a blastema is normally formed in animals with epimorphic regeneration – and appeared more abundant and directly confined at the correct location of missing structures, at later stages of regeneration where they differentiated in place.

Cell proliferation is required for ctenophore regeneration

Having demonstrated that cell proliferation is activated during ctenophore regeneration, our next aim was to address the requirement of cell proliferation in the process of regeneration. Juvenile cydippids were exposed to hydroxyurea (HU) treatments, a drug that inhibits cell proliferation by blocking the ribonucleotide reductase enzyme and thereby preventing the S-phase of cell cycle (Young and Hodas, 1964). We first performed a dose-response test experiment in order to set the working concentration of HU in which animals could be continuously incubated during the complete period of regeneration with no significant alterations/disruption of their fitness. Concentrations of 20, 10 and 5mM HU were tested over a 72-hour time course. Incubations in 20 and 10mM HU were toxic and caused the degeneration and eventually death of most of the animals during the first 24 hours of incubation (data not shown). Incubations in 5mM HU were much more harmless; cydippids maintained a good condition with no cell death over the 72-hour time course. We therefore decided to set 5mM HU as the working concentration for the cell proliferation inhibitor experiments. We then assessed the efficacy of that drug concentration in blocking cell proliferation in intact cydippids. Intact cydippids were incubated in 5mM HU for 24 and 72 hours and then incubated for 15 minutes with EdU as previously described (**Figure 7A**). By 24 hours of HU incubation, there was no detectable incorporation of EdU as compared with control cydippids, which showed the characteristic pattern of cell proliferation described in **Figure 4** (**Figure 7B-C'**). Inhibition of cell proliferation was maintained 72 hours after continuous HU incubation, as shown by the total absence of EdU+ cells in treated cydippids (**Figure 7D-E'**). Finally, we evaluated the effect of the drug during regeneration in dissected cydippids. Cydippids bisected through the aboral-oral axis and cydippids in which apical organ was amputated were exposed to a continuous incubation of 5mM HU from 0 to 72 hours after surgery. None of the bisected cydippids had regenerated at 72 hours following HU treatment (n=75). Wound closure and healing occurred normally as shown by the continuous epidermal layer covering the wound, but no sign of formation of the missing structures (tentacle bulb and comb rows) was observed (**Figure 8D-E'**). Likewise, none of the amputated cydippids had regenerated the missing apical organ at 72 hours following HU treatment (n=55), although the wound had correctly healed (**Figure 8H-J'**). Although HU treated animals failed to regenerate any of their missing

structures, an aggregation of cells could be observed at the wound site (**Figures 8E and 8J'**). These accumulations of quite large round-shaped cells could correspond to undifferentiated cells ready to re-form the missing structures but not able to proceed due to the blocking of cell proliferation. Importantly, the absence of EdU incorporation in dissected cydippids treated with HU confirmed that cell proliferation was completely suppressed by the HU incubation (**Figure 7I-J'**). From these observations we concluded that regeneration was impaired due to the absence of cell proliferation, therefore, cell proliferation is indispensable for ctenophore regeneration to proceed in a normal way.

Regenerative ability is recovered after HU treatment ends

Hydroxyurea has been shown to be reversible in cell culture following removal of the inhibitor (Adams and Lindsay, 1967) (**Figure 9A**). HU treatments on dissected cydippids showed that wound healing occurs normally without cell division. In order to determine whether regeneration could be initiated in HU treated animals we took dissected cydippids that had been exposed to HU over 48 hours, washed them in 1x filtered sea water (1x FSW) to remove the inhibitor, and then followed their development for 48 hours to check for regeneration (**Figures 9B and 9E**). Surprisingly, 36 out of 94 bisected cydippids (38%) regenerated all the missing structures (comb rows, tentacle bulb and tentacle) 48 hrs after HU treatment (**Figure 9D-D''**). 58 out of 94 bisected cydippids (62%) showed some signs of regeneration but ultimately remained as "half animals", suggesting that these animals were not healthy enough to complete the regeneration process (Bading et al., 2017). On the other hand, 100% of the cydippids in which the apical organ was surgically removed and had been treated with HU for 48 hours regenerated all the normal cell types of the apical organ (n=51) (**Figure 9H-I'**). Moreover, bisected cydippids in which HU was added 4 hab (n=25) – when wound healing is already completed – and 12 hab (n=25) – when cells at the wound site have already begun to cycle – fail to regenerate the missing structures (data not shown). Altogether, these results show that ctenophore regeneration can be initiated over 48 hours after wound healing is complete, hence, wound healing and regeneration appear to be two relatively independent events which can take place separately in time.

Proliferating cells from the uncut tissue migrate to the wound site

To investigate the source of cells that contribute to the formation of new tissue during ctenophore regeneration we performed a series of EdU pulse-chase experiments in regenerating cydippids. Uncut cydippids were incubated in EdU, which was incorporated into cells undergoing the S-phase of cell cycle. After a 15-minute pulse, EdU incorporation was blocked with several washes of thymidine and 1x FSW. Following the

washes, animals were amputated from the apical organ and let regenerate in 1x FSW (**Figure 10A**). The location of EdU+ cells was subsequently visualized at 48hpa. In combination to EdU detection, an immunostaining against PH3 was performed in order to detect cells that were actively dividing in the animal immediately before fixation. EdU+ cells were detected at the regenerated apical organ at 48hpa (n=11) (**Figure 10B-C'**). In a whole-body scale, the number of EdU+ nuclei had considerably increased compared to controls, specially at the areas of the pharynx, comb rows and mesoglea (**Supplementary Figure 4**). This general increment in EdU labeling could be the result of subsequent divisions of the original population of nuclei which had incorporated EdU during the 15-minute pulse. In addition, PH3+ cells were observed in the new apical organ tissue indicating active cell division at the moment of fixation (**Figure 10C-C'**). In an attempt to determine whether EdU+ cells at the regenerated apical organ continued dividing after migrating to the wound site, a thermal LUT was applied to the EdU-channel confocal projections as a way to qualitatively measure pixel intensity. According to this analysis, cells that did not divide or divided a very limited number of times would present a high pixel intensity, whereas cells that went through multiple rounds of division would show a very weak EdU staining, corresponding to lower pixel intensities by dilution of EdU through semi conservative DNA replication. Nuclei with EdU staining in all the range of pixel intensities were observed at the regenerating apical organ, however most EdU+ nuclei appeared in the intermediate intensities. Overall, the presence of EdU+ nuclei at the regenerated structures shows that proliferative cells originated in the pre-existing tissue migrate to the wound site and contribute to the formation of new tissue.

DISCUSSION

In this study, we provide detailed morphological and cellular characterization of wound healing and regeneration in the ctenophore *Mnemiopsis leidyi*. Wound closure is initiated immediately after injury, with the edges of the wound forming a round circumference that continues to reduce in diameter until they meet and forming a scar-less wound epithelium by 2 hours following injury. The wound healing process occurs normally in the absence of cell proliferation. This observation is consistent with the majority of animal models of regeneration found in the sister group of cnidarians (Singer, 1971; Passamaneck and Martindale, 2012; Bradshaw et al., 2015; Amiel et al., 2015). Following wound healing and prior to activation of cell proliferation, there is remodeling of the tissue surrounding the wound and small numbers of round-shaped cells sparsely congregate at the wound site suggesting a reorganization of the tissue in order to prepare it for regeneration. The cellular source of these early appearing cells is also unknown, although we provide some evidence from pulse chase EdU incorporation studies that at later stages of regeneration,

some cells might be migrating to the wound site from sources such as the tentacle bulb. Ctenophore regeneration, however, is strictly associated with epimorphic regeneration since none of the missing structures can be reformed in the absence of cell proliferation as proved by cell proliferation blocking treatments. Indeed, a combination of both epimorphosis and morphallaxis strategies has been previously described in the regeneration of other animals including annelids (De Jong and Seaver, 2016; Özpolat and Bely, 2016), although in those cases morphallaxis takes place simultaneously with epimorphosis – or even subsequent to epimorphosis – and is involved in the regeneration of a specific structures such as parapodia (Berril, 1931) or the gut (Zattara and Bely, 2011).

Cell proliferation in *M.* leidyi is first detected at the wound site around 6 hours after operation. The percentage of proliferating cells increases progressively during the first 12 hours following injury and reaches a maximum around 24 hours when the primordia of the missing structures are clearly delineated. Passed this peak of cell proliferation, the percentage of cell division decreases while cells start to differentiate into their final structures. Comparing the kinetics of cell proliferation during regeneration with the anthozoan cnidarian *Nematostella vectensis* (Passamaneck and Martindale, 2012), the percentage of dividing cells at the wound site is less numerous and the peak of maximum cell proliferation occurs earlier in ctenophore regeneration. In intact cydippids, cell proliferation is concentrated in two main areas of the cydippid's body corresponding to the tentacle bulbs. Some actively cycling cells are also found in the apical organ as well as few isolated dividing cells along the pharynx and under the comb rows. These results are consistent with previous EdU analysis performed in *Mnemiopsis* cydippids (Schnitzler et al., 2014; Reitzel et al., 2016) and adult ctenophores of the species *Pleurobrachia pileus* (Alié et al., 2011). Pulse-chase experiments show migration of proliferating cells from the tentacle bulb through the tentacle while a small population of dividing cells remains stable at the tentacle sheath. These observations fit with histological and cellular descriptions of the tentacle apparatus (Alié et al., 2011; Borisenko and Ereskovsky, 2013) which identified different populations of undifferentiated progenitors source of all cell types found in the tentacle tissue.

Interestingly, proliferating cells during regeneration do not organize to form a single large blastema-like structure from which a field of cells proliferate and differentiate to form the missing structures. Rather small numbers of undifferentiated cells assume the correct location of all missing structures simultaneously and differentiate in place. Considering the phylogenetic position of ctenophores in the tree of life (Dunn et al., 2008; Ryan et al., 2013), the absence of blastema during ctenophore regeneration questions whether the formation of a blastema – which so far appears to have been reported in

representatives of all phyla of regenerating animals (Sánchez Alvarado, 2000) – is a conserved trait among the evolution of regeneration.

The strict requirement of cell proliferation and the absence of blastema formation make ctenophore regeneration a case of non-blastemal epimorphic regeneration. Although far less common as the blastemal based regeneration, isolated cases of non-blastemal regeneration have been reported such as lens regeneration by transdifferentiation in newts (Tsonis and Del Rio-Tsonis, 2004) or liver regeneration by compensatory proliferation in humans (Michalopoulos and DeFrances, 1997). EdU pulse-chase experiments show contribution of proliferating cells from the pre-existing tissue to the formation of new tissue, but whether these cells are the result of stem cell proliferation or dedifferentiation/transdifferentiation events remains unclear. Expression of genes involved in stem cell maintenance and regulation of cell fate has been localized within zones of active cell proliferation (Alié et al., 2011; Schnitzler et al., 2014; Reitzel et al., 2016), suggesting the presence of stem cell niches that could act as the source of new tissue during regeneration. However, combination of cell linage experiments and specific cell deletion experiments showed that comb plate regeneration cannot occur when their cell lineage of progenitors are killed during embryogenesis, suggesting that at least for comb plate regeneration, a pluripotent somatic stem cell population set-aside during embryogenesis does exist not (Martindale and Henry, 1999, 1996). Rather, linage restricted progenitors seem to be the most plausible strategy for comb row formation during regeneration, suggesting that ctenophore regeneration resembles the amphibian mode of lineage restriction more closely than the planarian mode of pluripotent stem cells (Martindale, 2016). Differential gene expression analysis during the process of regeneration in *M. leidyi* will allow us to identify genes involved in stemness and differentiation. Molecular data during regeneration will also be very valuable for performing comparisons of gene expression profiles between *Mnemiopsis* development (Levin et al., 2016) and regeneration and thus determine whether the molecular basis of ctenophore regeneration is similar to that deployed during development.

It is quite accepted that cells that re-epithelialize the wound provide the signals necessary to initiate regeneration (Brockes and Kumar, 2008; Owlarn et al., 2017). In vertebrates, local thrombin activation is a signal for regeneration as shown by the study in which cultured newt myotubes returned to the cell cycle by the activity of a thrombin-generated ligand (Tanaka et al., 1999). On the other hand, cellular interactions also seem to be important for the initiation of the regenerative response. One such case is the dorsoventral interaction between the wounded tissues during wound healing in planarians which has been shown to play a key role in the formation of the blastema and, hence, initiation of regeneration (Kato et al., 1999). These observations suggest that

wound healing and regeneration are two closely related processes which need to take place sequentially in time. Our results, however, show that ctenophore regeneration can be initiated over 48 hours after wound healing is complete, suggesting that regeneration can be initiated without direct signaling induced by the wounded epithelium. Regeneration of the missing structures is not initiated until the cell proliferation blocking treatment is replaced. Hence, another possible explanation is that the wound epithelium produces signaling necessary for triggering regeneration at the time of wound healing, but the process cannot be initiated due to the blocking of cell proliferation. This is consistent with the proposed hypothesis for *Nematostella* that the key transition from wound healing to a state of regeneration is the activation of cell proliferation (DuBuc et al., 2014). Studying and comparing the molecular signaling involved in both ctenophore wound healing and regeneration will be very useful to get further insight into the relationship between these two processes.

In conclusion, this study provides a rigorous description of the morphological and cellular events during ctenophore regeneration and compare them with the regenerative strategies followed by other metazoans. The phylogenetic position of ctenophores together with their remarkable ability to regenerate make them a key model system to grow more knowledge in to the understanding of the evolution of animal regeneration.

REFERENCES

Adams, R.L.P., Lindsay, J.., 1967. Hydroxyurea. Reversal of inhibition and use as a cell-synchronizing agent. J. Biol. Chem. 242, 1314–1317.

Alejandro Sánchez, A., 2000. Regeneration in the metazoans: why does it happen? BioEssays 22, 578–590.

Alié, A., Leclère, L., Jager, M., Dayraud, C., Chang, P., Le Guyader, H., Quéinnec, E., Manuel, M., 2011. Somatic stem cells express Piwi and Vasa genes in an adult ctenophore: Ancient association of “germline genes” with stemness. Dev. Biol. 350, 183–197. https://doi.org/10.1016/j.ydbio.2010.10.019

Alvarado, A.S., Tsonis, P.A., 2006. Bridging the regeneration gap: Genetic insights from diverse animal models. Nat. Rev. Genet. 7, 873–884. https://doi.org/10.1038/nrg1923

Amiel, A.R., Johnston, H.T., Nedoncelle, K., Warner, J.F., Ferreira, S., Röttinger, E., 2015. Characterization of morphological and cellular events underlying oral regeneration in the sea anemone, Nematostella vectensis. Int. J. Mol. Sci. 16, 28449–28471. https://doi.org/10.3390/ijms161226100

Bading, K.T., Kaehlert, S., Chi, X., Jaspers, C., Martindale, M.Q., Javidpour, J., 2017. Food availability drives plastic self-repair response in a basal metazoan-case

study on the ctenophore Mnemiopsis leidyi A. Agassiz. Sci. Rep. 7, 1–9. https://doi.org/10.1038/s41598-017-16346-w

Baguna, J., Salo, E., Auladell, C., 1989. Regeneration and pattern formation in planarians. III. that neoblasts are Regeneration and pattern formation in planarians. III. that neoblasts are totipotent stem cells and the cells totipotent stem cells and the cells. Development 107, 77–86.

Bely, A.E., 2014. Early events in annelid regeneration: a cellular perspective. Integr. Comp. Biol. 54, 688–699. https://doi.org/10.1093/icb/icu109

Bely, A.E., Nyberg, K.G., 2010. Evolution of animal regeneration: re-emergence of a field. Trends Ecol. Evol. 25, 161–170. https://doi.org/10.1016/j.tree.2009.08.005

Berrill NJ, 1931. Regeneration in Sabella pavonina (Sav.) and other sabellid worms. J Exp Zool. 58:495-523.

Borisenko, I., Ereskovsky, A. V., 2013. Tentacular apparatus ultrastructure in the larva of Bolinopsis infundibulum (Lobata: Ctenophora). Acta Zool. https://doi.org/10.1111/j.1463-6395.2011.00542.x

Bradshaw, B., Thompson, K., Frank, U., 2015. Distinct mechanisms underlie oral vs aboral regeneration in the cnidarian hydractinia echinata. Elife 2015, 1–19. https://doi.org/10.7554/eLife.05506

Brockes, J.P., Kumar, A., 2008. Comparative Aspects of Animal Regeneration. Annu. Rev. Cell Dev. Biol. 24, 525–549. https://doi.org/10.1146/annurev.cellbio.24.110707.175336

Chehrehasa, F., Meedeniya, A.C.B., Dwyer, P., Abrahamsen, G., Mackay-Sim, A., 2009. EdU, a new thymidine analogue for labelling proliferating cells in the nervous system. J. Neurosci. Methods 177, 122–130. https://doi.org/10.1016/j.jneumeth.2008.10.006

Coonfield, B.R., 1936. Regeneration in Mnemiopsis Leidyl Agassiz. Biol. Bull. 71, 421–428.

Cummings, S.G., Bode, H.R., 1984. Head regeneration and polarity reversal in Hydra attenuata can occur in the absence of DNA synthesis. Wilhelm Roux's Arch. Dev. Biol. 194, 79–86. https://doi.org/10.1007/BF00848347

De Jong, D.M., Seaver, E.C., 2016. A Stable Thoracic Hox Code and Epimorphosis Characterize Posterior Regeneration in Capitella teleta. PLoS One 11. https://doi.org/10.1371/journal.pone.0149724

De Jong, D.M., Seaver, E.C., 2017. Investigation into the cellular origins of posterior regeneration in the annelid *Capitella teleta*. Regeneration 1–17. https://doi.org/10.1002/reg2.94

Dübel, S., Schaller, H.C., 1990. Terminal Differentiation of Ectodermal Epithelial Stem

Cells of Hydra Can Occur in G2 without Requiring Mitosis or S Phase. J. Cell Biol. 110, 939–945. https://doi.org/10.1083/jcb.110.4.939

DuBuc, T.Q., Traylor-Knowles, N., Martindale, M.Q., 2014. Initiating a regenerative response; cellular and molecular features of wound healing in the cnidarian Nematostella vectensis. BMC Biol. 12, 1–20. https://doi.org/10.1186/1741-7007-12-24

Dunn, C.W., Hejnol, A., Matus, D.Q., Pang, K., Browne, W.E., Smith, S.A., Seaver, E., Rouse, G.W., Obst, M., Edgecombe, G.D., Sørensen, M. V., Haddock, S.H.D., Schmidt-Rhaesa, A., Okusu, A., Kristensen, R.M., Wheeler, W.C., Martindale, M.Q., Giribet, G., 2008. Broad phylogenomic sampling improves resolution of the animal tree of life. Nature 452, 745–749. https://doi.org/10.1038/nature06614

Fischer, A.H.L., Pang, K., Henry, J.Q., Martindale, M.Q., 2014. A cleavage clock regulates features of lineage-specific differentiation in the development of a basal branching metazoan, the ctenophore Mnemiopsis leidyi. Evodevo 5. https://doi.org/10.1186/2041-9139-5-4

Freeman, G., 1967. Studies on regeneration in the creeping ctenophore, Vallicula multiformis. J. Morphol. https://doi.org/10.1002/jmor.1051230107

Henry, J.Q., Martindale, M.Q., 2000. Regulation and regeneration in the ctenophore Mnemiopsis leidyi. Dev. Biol. 227, 720–733. https://doi.org/10.1006/dbio.2000.9903

Holstein, T.W., Hobmayer, E., David, C.N., 1991. Pattern of epithelial cell cycling in hydra. Dev. Biol. 148, 602–611. https://doi.org/10.1016/0012-1606(91)90277-A

Jager, M., Manuel, M., 2016. Ctenophores: an evolutionary-developmental perspective. Curr. Opin. Genet. Dev. 39, 85–92. https://doi.org/10.1016/j.gde.2016.05.020

Kato, K., Orii, H., Watanabe, K., Agata, K., 1999. The role of dorsoventral interaction in the onset of planarian regeneration. Development 126, 1031–1040. https://doi.org/10.1242/dev.031682

Kragl, M., Knapp, D., Nacu, E., Khattak, S., Maden, M., Epperlein, H.H., Tanaka, E.M., 2009. Cells keep a memory of their tissue origin during axolotl limb regeneration. Nature 460, 60–65. https://doi.org/10.1038/nature08152

Levin, M., Anavy, L., Cole, A.G., Winter, E., Mostov, N., Khair, S., Senderovich, N., Kovalev, E., Silver, D.H., Feder, M., Fernandez-Valverde, S.L., Nakanishi, N., Simmons, D., Simakov, O., Larsson, T., Liu, S.-Y., Jerafi-Vider, A., Yaniv, K., Ryan, J.F., Martindale, M.Q., Rink, J.C., Arendt, D., Degnan, S.M., Degnan, B.M., Hashimshony, T., Yanai, I., 2016. The mid-developmental transition and the evolution of animal body plans. Nature 531, 637.

Martindale, M.Q., 1986. The ontogeny and maintenance of adult symmetry properties

in the ctenophore, Mnemiopsis mccradyi. Dev. Biol. https://doi.org/10.1016/0012-1606(86)90026-6

Martindale, M.Q., 2016. The onset of regenerative properties in ctenophores. Curr. Opin. Genet. Dev. 40, 113–119. https://doi.org/10.1016/j.gde.2016.06.017

Martindale, M.Q., Henry, J.Q., 1996. Development and Regeneration of Comb Plates in the Ctenophore Mnemiopsis leidyi. Biol. Bull. 191, 290–292. https://doi.org/10.1086/BBLv191n2p290

Martindale, M.Q., Henry, J.Q., 1999. Intracellular Fate Mapping in a Basal Metazoan, the Ctenophore Mnemiopsis leidyi, Reveals the Origins of Mesoderm and the Existence of Indeterminate Cell Lineages. Dev. Biol. 214, 243–257.

Michalopoulos, G.K., DeFrances, M., 1997. Liver regeneration. Science (80-.). 276, 60–66. https://doi.org/10.1007/b99968

Morgan, T.H., 1901. Regeneration. New York: The Macmillan Company.

Newmark, P.A., Sánchez Alvarado, A., 2000. Bromodeoxyuridine specifically labels the regenerative stem cells of planarians. Dev. Biol. 220, 142–153. https://doi.org/10.1006/dbio.2000.9645

Owlarn, S., Klenner, F., Schmidt, D., Rabert, F., Tomasso, A., Reuter, H., Mulaw, M.A., Moritz, S., Gentile, L., Weidinger, G., Bartscherer, K., 2017. Generic wound signals initiate regeneration in missing-tissue contexts. Nat. Commun. 8, 1–13. https://doi.org/10.1038/s41467-017-02338-x

Özpolat, B.D., Bely, A.E., 2016. Developmental and molecular biology of annelid regeneration: a comparative review of recent studies. Curr. Opin. Genet. Dev. 40, 144–153. https://doi.org/10.1016/j.gde.2016.07.010

Pang, K., Martindale, M.Q., 2008. Comb jellies (Ctenophora): A model for basal metazoan evolution and development. Cold Spring Harb. Protoc. 3, 1–11. https://doi.org/10.1101/pdb.emo106

Park, H.D., Ortmeyer, A.B., Blankenbaker, D.P., 1970. Cell Division during Regeneration in Hydra. Nature 228, 227–231.

Passamaneck, Y.J., Martindale, M.Q., 2012. Cell proliferation is necessary for the regeneration of oral structures in the anthozoan cnidarian Nematostella vectensis. BMC Dev. Biol. 12. https://doi.org/10.1186/1471-213X-12-34

Reitzel, A.M., Pang, K., Martindale, M.Q., 2016. Developmental expression of “germline”- and “sex determination”-related genes in the ctenophore Mnemiopsis leidyi. Evodevo 7, 1–16. https://doi.org/10.1186/s13227-016-0051-9

Ryan, J.F., Pang, K., Schnitzler, C.E., Nguyen, A.D., Moreland, R.T., Simmons, D.K., Koch, B.J., Francis, W.R., Havlak, P., Smith, S.A., Putnam, N.H., Haddock, S.H.D., Dunn, C.W., Wolfsberg, T.G., C.Mullikin, J., Martindale, M.Q., Baxevanis,

A.D., 2013. The genome of the ctenophore Mnemiopsis leidyi and its implications for cell type evolution. Science (80-.). 342. https://doi.org/10.1126/science.1242592

Salic, A., Mitchison, T.J., 2008. A chemical method for fast and sensitive detection of DNA synthesis in vivo. PNAS 105. https://doi.org/10.1073/pnas.0712168105

Salinas-Saavedra, M., Martindale, M.Q., 2018. Improved protocol for spawning and immunostaining embryos and juvenile stages of the ctenophore _Mnemiopsis leidyi_.

Sánchez Alvarado, A., 2000. Regeneration in the metazoans: why does it happen? BioEssays 22, 578–590.

Schnitzler, C.E., Simmons, D.K., Pang, K., Martindale, M.Q., Baxevanis, A.D., 2014. Expression of multiple Sox genes through embryonic development in the ctenophore Mnemiopsis leidyi is spatially restricted to zones of cell proliferation. Evodevo 5, 1–17. https://doi.org/10.1186/2041-9139-5-15

Singer, I.I., 1971. Tentacular and oral-disc regeneration in the sea anemone, Aiptasia diaphana. J. Embryol. Exp. Morphol. 26, 253–270. https://doi.org/10.1007/BF00597293

Tamm SL, 2012. Regeneration of ciliary comb plates in the ctenophore Mnemiopsis leidyii morphology. J Morph. 273:109-120.

Tanaka, E.M., Drechsel, D.N., Brockes, J.P., 1999. Thrombin regulates S-phase re-entry by cultured newt myotubes. Curr. Biol. 9, 792–799. https://doi.org/10.1016/S0960-9822(99)80362-5

Tanaka, E.M., Reddien, P.W., 2011. The Cellular Basis for Animal Regeneration. Dev. Cell 21, 172–185. https://doi.org/10.1016/j.devcel.2011.06.016

Tsonis, P.A., Del Rio-Tsonis, K., 2004. Lens and retina regeneration: Transdifferentiation, stem cells and clinical applications. Exp. Eye Res. 78, 161–172. https://doi.org/10.1016/j.exer.2003.10.022

Wagner, D.E., Wang, I.E., Reddien, P.W., 2011. Clonogenic neoblasts are pluripotent adult stem cells that underlie planarian regeneration. Science (80-.). 332, 811–816. https://doi.org/10.1126/science.1203983.

Young CW, Hodaas S, 1964. Hydroxyurea: inhibitory effect on DNA metabolism. Science. 146:1172–1174.

Zattara, E.E., Bely, A.E., 2011. Evolution of a novel developmental trajectory: Fission is distinct from regeneration in the annelid Pristina leidyi. Evol. Dev. 13, 80–95. https://doi.org/10.1111/j.1525-142X.2010.00458.x

Zattara, E.E., Turlington, K.W., Bely, A.E., 2016. Long-term time-lapse live imaging reveals extensive cell migration during annelid regeneration. BMC Dev. Biol. 16,

1–21. https://doi.org/10.1186/s12861-016-0104-2

FIGURE LEGENDS

Figure 1. Animal surgeries. Diagrams illustrating the two types of operations performed in this study: 1) Oral-aboral bisection and 2) Apical organ amputation.

Figure 2. Half body regeneration in *Mnemiopsis leidyi cydippid*. (**A**) Schematic representation of the time course of morphogenic events during cydippid half body regeneration. All cartoons correspond to lateral views of the cydippid's body bisected through the oral-aboral axis showing the cut site in the first plane. The apical organ is located at the aboral end (top) and the mouth at the oral end (down). For simplicity, tissues on the opposite body site are not depicted. (**B-F**) DIC images showing the cut site of regenerating cydippids from 16 to 96 hab. Dotted line rectangles in (**B**), (**C**), (**D**) and (**E**) show the area corresponding to higher magnifications on the right. Magnifications show surface and deep planes. The vertical dotted line in (**F**) indicates the approximate position of bisection, and all tissue in the left of the line is regenerated tissue. The scale bar in all panels represents 100 μm. Abbreviations: hours after bisection (h a.b.), apical organ (a.o.), pharynx (p), comb row (c.r.), ciliated furrow (c.f.), comb plate (c.p.), tentacle bulb (t.b.), tentacle (t).

Figure 3. Apical organ regeneration in *Mnemiopsis leidyi* cydippids. (**A**) Schematic representation of the time course of morphogenic events during cydippid's apical organ regeneration. Cartoons correspond to lateral views of the apical sensory organ at different stages of regeneration. (**B-C'**) DIC images of the apical organ of an intact cydippid in lateral (**B-B'**) and aboral (**C-C'**) views. (**D-D**) Schematic of the components of the apical sensory organ in lateral (**D**) and aboral (**D'**) views. (**E-L'**) DIC images showing the cut site of regenerating cydippids after apical organ amputation from 12 to 60 hpa. Lateral and aboral views are included. Dotted line rectangles delimit the area corresponding to higher magnifications on the right. Filled and empty white arrow caps in (**G'**) point to aggregation of cells forming the primordia of the future statolith and apical organ floor respectively. The scale bar in all panels represents 100 μm. Abbreviations: hours post amputation (h p.a.), dome cilia (d.c.), lithocyte (l), supporting cilia (s.c.), apical organ floor (a.o. fl.), endodermal canal (e.c.), ciliated furrows (c.f.).

Figure 4. Cell proliferation in intact cydippids. (**A**) Schematic of the EdU pulse-chase experiment and PH3 immunostaining in intact cydippids. (**B-D'**) Confocal stack projections of whole intact cydippids oriented in a lateral view. White dotted rectangles

in (**B)** delimit the tentacle bulb (t.b.) (**C-C'''**) and apical organ (a.o.) (**D-D'''**) structures showed in higher magnification at the bottom. Nuclei of S-phase cells are labeled with EdU (magenta), M-phase cells are immunostained with anti-phospho-Histone 3 (PH3) (green) and all nuclei are counterstained with DAPI (blue). Note that both markers of cell proliferation (EdU and PH3) show the same pattern of distribution along the cydippid's body. (**E-G'**) Confocal stack projections of whole intact cydippids oriented in a lateral view. The time of the chase is listed at the top of the columns, and the labeling corresponding to each panel is listed to the left of the rows. Nuclei of S-phase cells are labeled with EdU (magenta) and all nuclei are counterstained with DAPI (blue). Note that EdU+ cells migrate from the tentacle bulb to the most distal end of the tentacle. (**H-K'**) Confocal stack projections of tentacle bulbs and tentacles in lateral view. The time of the chase is listed to the left of the rows, and the labeling corresponding to each panel is listed at the top of the columns. Nuclei of S-phase cells are labeled with EdU (magenta) combined with a differential interference contrast image of the tissue (DIC). Scale bars represent 100μm in panels (**B-G'**) and 50μm in panels (**H-K'**).

Figure 5. Cell proliferation during half body regeneration. (**A**) Schematic of the EdU incorporation experiment in cydippids bisected through the oral-aboral axis. (**B-I'**) Confocal stack projections of bisected cydippids through the oral-aboral axis oriented in a lateral view showing the cut site in the first plane. The time following bisection is listed at the top of the columns, and the labeling corresponding to each panel is listed to the left of the rows. Nuclei of S-phase cells are labeled with EdU (magenta) and all nuclei are counterstained with DAPI (blue). Cartoons in (**B'**), (**C'**), (**D'**), (**F'**) and (**H'**) show the orientation of the animals with the pattern of EdU labeling corresponding to each stage of regeneration. Dotted line rectangles in (**D**), (**F**) and (**H**) show the area corresponding to higher magnifications on the right. White dotted lines in (**G-G'**) and (**I-I'**) delimit the area corresponding to the regenerating comb rows and tentacle bulb. White asterisks point to tentacle bulbs of the uncut site. Scale bars in all panels represent 100 μm. Abbreviations: hours after bisection (h a.b.) comb row (c.r.), tentacle bulb (t.b.).

Figure 6. Cell proliferation during apical organ regeneration. (**A**) Schematic of the EdU incorporation experiment and PH3 immunostaining in cydippids amputated from the apical organ. (**B**) Graph showing the levels of cell proliferation at the wound site at different time points post amputation. (**C-H''**) Confocal stack projections of amputated cydippids from the apical organ at different time points post amputation. Aboral and lateral views are shown. The labeling corresponding to each panel is listed at the top of the columns, and the time following amputation is listed to the left of the rows. Dotted

line rectangles in (**C**), (**D**), (**E**), (**F**), (**G**) and (**H**) show the area corresponding to higher magnifications on the right. White rectangles in (**C''**) and (**D''**) delimit the area of apical organ regeneration. Nuclei of S-phase cells are labeled with EdU (magenta) and all nuclei are counterstained with DAPI (blue). DIC images of the tissue are shown in (**F'**) and (**H'**). (**I-I''**) M-phase cells in the regenerating apical organ stained with anti-PH3 (green) at 24 hpa. DIC images of surface and deep planes are shown. Scale bars in all panels represent 100 μm. Abbreviations: hours post amputation (h p.a.), phospho Histone-3 (PH3).

Figure 7. 5mM Hydroxyurea (HU) blocks cell proliferation in intact and bisected cydippids. (**A**) Schematic of cell proliferation inhibitor experiments with HU in intact cydippids. (**B-C'**) Confocal stack projections of intact cydippids oriented in an aboral view at 24 hours after HU incubation. (**D-E'**) Confocal stack projections of intact cydippids oriented in a lateral view at 72 hours after HU incubation. The type of treatment is listed at the top of the columns, and the labeling corresponding to each panel is listed to the left of the rows. Nuclei of S-phase cells are labeled with EdU (magenta) and all nuclei are counterstained with DAPI (blue). Note that no EdU+ nuclei were detected in treated cydippids after HU incubation. (**F**) Schematic of cell proliferation inhibitor experiments with HU in dissected cydippids. (**G-H'**) Confocal stack projections of an untreated bisected cydippid oriented in a in lateral view at 72 hab. (**I-I**') Confocal stack projections of a bisected cydippids treated with HU at 72 hab. (**J-J'**) Confocal stack projections of cydippids amputated from the apical organ treated with HU at 72 hpa. The type of treatment and the time following bisection are listed at the top of the columns, and the labeling corresponding to each panel is listed to the left of the rows. The dotted line rectangle in (**G**) shows the area corresponding to higher magnifications on the right. The white asterisks in (**G**), (**G'**) and (**I**) point to the tentacle bulb of the uncut site. The white rectangle in (**J**) indicates the area of apical organ regeneration. Nuclei of S-phase cells are labeled with EdU (magenta) and all nuclei are counterstained with DAPI (blue). Note that no EdU+ nuclei were detected and none of the missing structures regenerated in treated cydippids. Scale bars in all panels represent 100 μm. Abbreviations: hours after bisection (h a.b.), hours post amputation (h p.a.).

Figure 8. Ctenophore regeneration does not occur in the absence of cell proliferation. (**A**) Schematic representation of the regeneration state of cydippids shown in the panels on the right. Cartoons correspond to lateral views of the cydippid's body bisected in half through the oral-aboral axis showing the cut site in the first plane. (**B-E'**) DIC images of bisected cydippids in a lateral view at 72 hab. The type of treatment

corresponding to each panel is listed to the left of the rows. Dotted line rectangles in (**B**) and (**D**) show the area corresponding to higher magnifications on the right. Magnifications show surface (top) and deep (bottom) planes. Note that the wound site in treated cydippids is covered by a continuous epithelium but there is no sign of formation of missing structures. (**F**) Schematic representation of the apical sensory organ in lateral (top) and aboral (bottom) views. Red dotted rectangle at the bottom cartoon delimits the apical organ area shown in the images on the right. (**G-H'**) DIC images of cydippids amputated from the apical organ at 72 hpa orientated in a lateral view. (**I-J'**) DIC images of cydippids amputated from the apical organ at 72 hpa orientated in an aboral view. The type of treatment corresponding to each panel is listed to the top of the columns. Dotted line rectangles in (**G**), (**H**), (**I**) and (**J**) show the area corresponding to higher magnifications on the bottom. Note that treated cydippids show aggregation of cells around the surface of the wounded area although none of the missing apical organ structures are formed. The scale bar in all panels represents 100 μm. Abbreviations: hours after bisection (h a.b.), hours post amputation (h p.a.), apical organ (a.o.), comb row (c.r.), tentacle bulb (t.b.), statolith (s), cupula (c), apical organ floor (a.o. fl.), endodermal canal (e.c.), lithocyte (l), ciliated furrow (c.f.).

Figure 9. Regenerative ability is recovered after HU treatment ends. (**A**) Reversible S-phase arrest after HU treatment as detected by EdU labeling performed at the indicated time-points (red arrows). Nuclei of S-phase cells are labeled with EdU (magenta) and all nuclei are counterstained with DAPI (blue). The dotted line rectangle shows the area corresponding to higher magnifications on the right. Note that cells have already resumed cell cycle progression 1 day after HU wash (**B**) Schematic representation of HU treatment and wash experiment in bisected cydippids through the oral-aboral axis. (**C-C'**) DIC images of bisected cydippids in lateral view showing the wound site at 48 hab (just after HU treatment and before washing). The dotted line rectangle in (**C**) shows the area corresponding to higher magnification at the bottom. Note that there is no sign of regeneration of the missing structures. (**D**-**D''**) DIC images of bisected cydippids in lateral view showing the wound site at 96 hab (48h after HU wash). The dotted line rectangle in (**D**) shows the area corresponding to higher magnification at the bottom. Note that all missing structures (comb rows and tentacle bulb) are regenerated. (**E**) Schematic representation of HU treatment and wash experiment in cydippids in which the apical organ was amputated. (**F-G'**) DIC images of amputated cydippids oriented in a lateral (top panels) and aboral (bottom panels) view showing the wound site at 48 hpa (just after HU treatment and before washing). Dotted line rectangles in (**F**) and (**G**) shows the area corresponding to higher magnification on

the right. Note that there is no sign of regeneration of the missing structures. (**H-I'**) DIC images of amputated cydippids oriented in a lateral (top panels) and aboral (bottom panels) view showing the wound site at 96 hpa (48h after HU wash). Dotted line rectangles in (**H**) and (**I**) show the area corresponding to higher magnification on the right. Note that all components of the apical organ are regenerated. The scale bar in all panels represents 100 μm. Abbreviations: hours after bisection (h a.b.), hours post amputation (h p.a.), apical organ (a.o.), comb row (c.r.), tentacle bulb (t.b.), dome cilia (d.c.), lithocyte (l), supporting cilia (s.c.), apical organ floor (a.o. fl.), endodermal canal (e.c.), ciliated furrows (c.f.).

Figure 10. Proliferating cells from the uncut tissue migrate to the wound site (**A**) Schematic representation of EdU pulse-chase experiments and PH3 immunostaining in regenerating cydippids amputated from the apical organ. (**B-C'''**) Confocal stack projections of regenerating apical organ oriented in a lateral (**B-B'''**) and aboral (**C-C'''**) view at 48 hpa. Nuclei of S-phase cells are labeled with EdU (magenta), M-phase cells are immunostained with anti-phospho-Histone 3 (PH3) (green) and all nuclei are counterstained with DAPI (blue). (**D-D'**) Thermal LUT taken from the EdU channel of the same specimens shown in (**B'**) and (**C'**). The Thermal LUT scale bar indicates pixel intensity. The scale bar in all panels represents 100μm.

FIGURE SUPPLEMENTS

Figure supplement 1. EdU staining in a bisected cydippid at 96 hab. Confocal stack projections of a bisected cydippid through the oral-aboral axis oriented in a lateral view showing the cut site in the first plane. Nuclei of S-phase cells are labeled with EdU (magenta) and all nuclei are counterstained with DAPI (blue). Dotted line rectangle show the area including the regenerated comb rows and tentacle bulb, corresponding to higher magnifications on the right. Scale bar: 100μm.

Figure supplement 2. PH3 immunostaining in amputated cydippid at 48 hpa. Confocal stack projections of amputated cydippids from the apical organ at 48 hpa. M-phase cells in the regenerating apical organ stained with anti-PH3 (green) combined with DIC image of the tissue. Scale bar: 100μm.

Figure supplement 3. Controls of the EdU pulse-chase experiments in regenerating cydippids. (**A**) Diagram of the experimental setup. (**B-D'**) Confocal stack projections of an uncut cydippid just after EdU incubation (control 1). (**E-F'**) Confocal

stack projections of an amputated cydippid just after the cut (control 2). Nuclei of S-phase cells are labeled with EdU (magenta) and all nuclei are counterstained with DAPI (blue). White dotted rectangles in (**B**) and (**E**) show the area corresponding to higher magnifications on the right. White arrows in (E') point to the wound site. Scale bar: 100μm.

Figure supplement 4. EdU pulse-chase experiment and PH3 immunostaining in whole-body of an amputated cydippid. Confocal stack projections of a cydippid amputated from the apical organ oriented in a lateral view at 48hpa. Nuclei of S-phase cells are labeled with EdU (magenta), M-phase cells are immunostained with anti-phospho-Histone 3 (PH3) (green) and all nuclei are counterstained with DAPI (blue). Scale bar: 100μm.

Figure 1

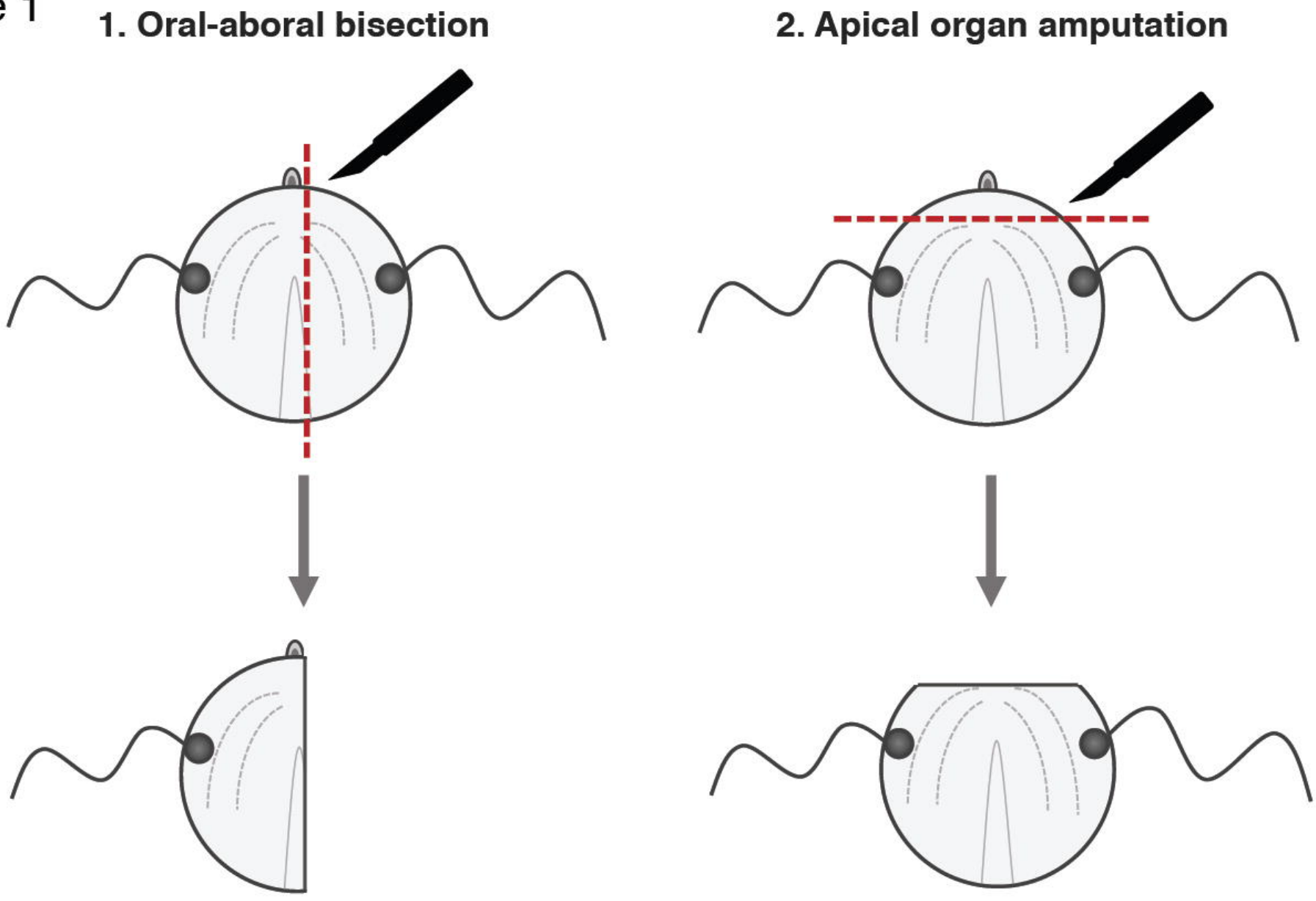

Figure 2

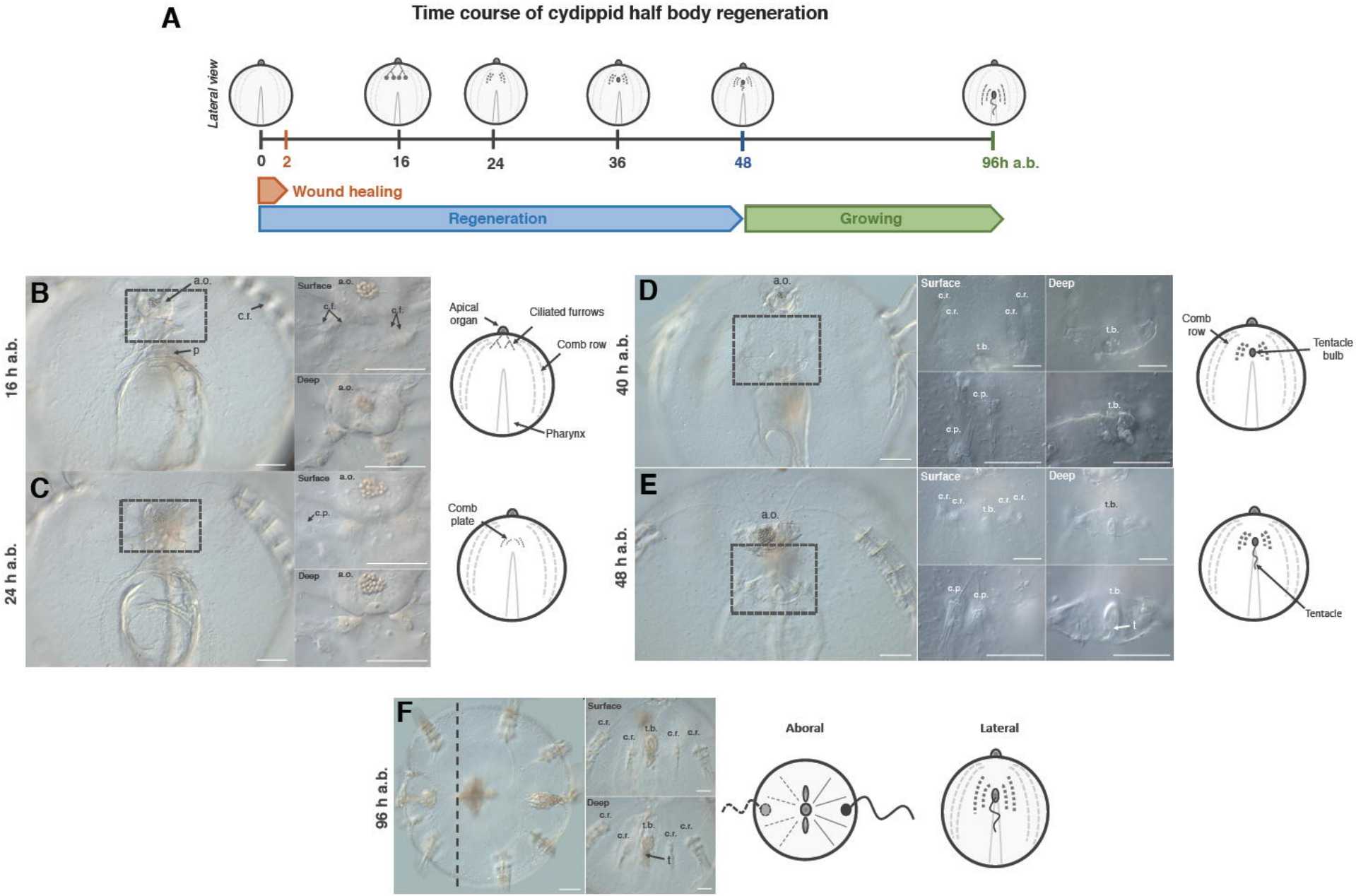
A
Time course of cydippid half body regeneration
Lateral view
0
2
16
24
36
48
96h a.b.
Wound healing
Regeneration
Growing
B
16 h a.b.
a.o.
c.r.
p
Surface
c.f.
Deep
Apical organ
Ciliated furrows
Comb row
Pharynx
C
24 h a.b.
c.p.
Comb plate
D
40 h a.b.
t.b.
Comb row
Tentacle bulb
E
48 h a.b.
t
Tentacle
F
96 h a.b.
Aboral
Lateral

Figure 3

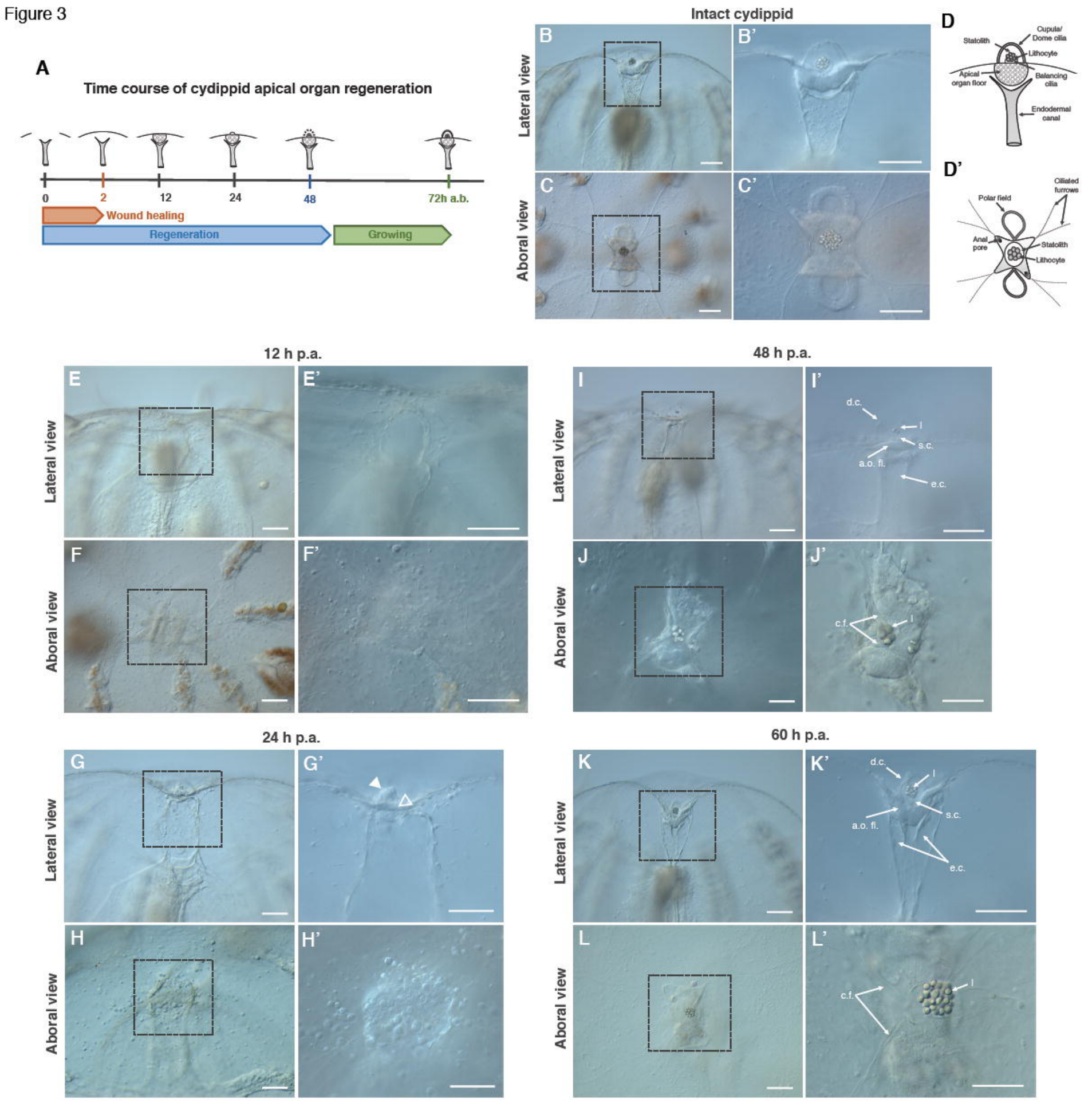
A
Time course of cydippid apical organ regeneration
0
2
12
24
48
72h a.b.
Wound healing
Regeneration
Growing
Intact cydippid
Lateral view
Aboral view
B
B'
C
C'
D
Cupula/ Dome cilia
Statolith
Lithocyte
Apical organ floor
Balancing cilia
Endodermal canal
D'
Ciliated furrows
Polar field
Anal pore
Statolith
Lithocyte
12 h p.a.
E
E'
F
F'
48 h p.a.
I
I'
d.c.
l
s.c.
a.o. fl.
e.c.
J
J'
c.f.
24 h p.a.
G
G'
H
H'
60 h p.a.
K
K'
L
L'

Figure 4

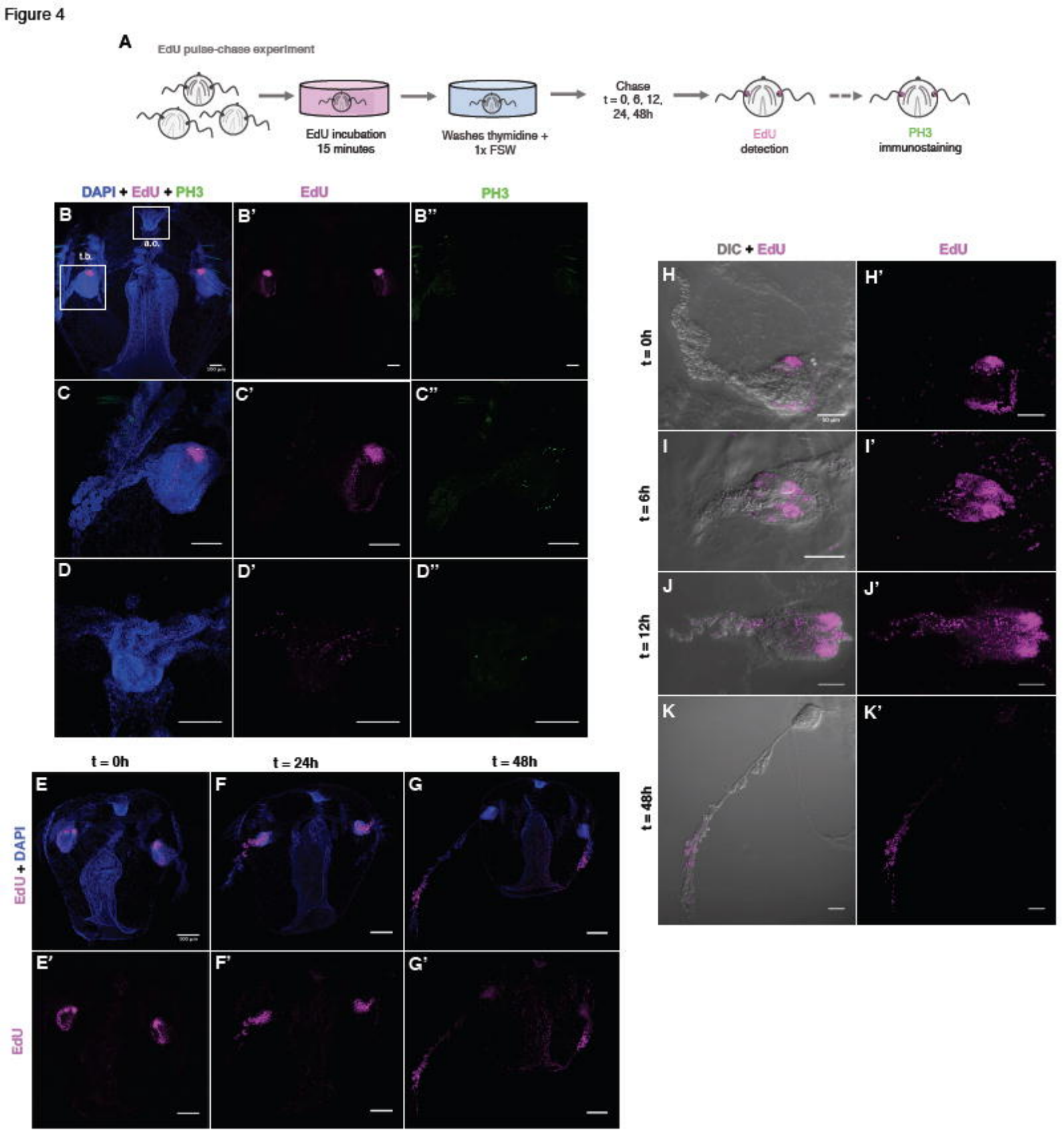
A
EdU pulse-chase experiment
EdU incubation
15 minutes
Washes thymidine +
1x FSW
Chase
t = 0, 6, 12,
24, 48h
EdU
detection
PH3
immunostaining
DAPI + EdU + PH3
EdU
PH3
B
B'
B''
a.o.
t.b.
C
C'
C''
D
D'
D''
DIC + EdU
EdU
H
H'
I
I'
J
J'
K
K'
t = 0h
t = 6h
t = 12h
t = 48h
t = 0h
t = 24h
t = 48h
E
F
G
E'
F'
G'
EdU + DAPI
EdU

Figure 5

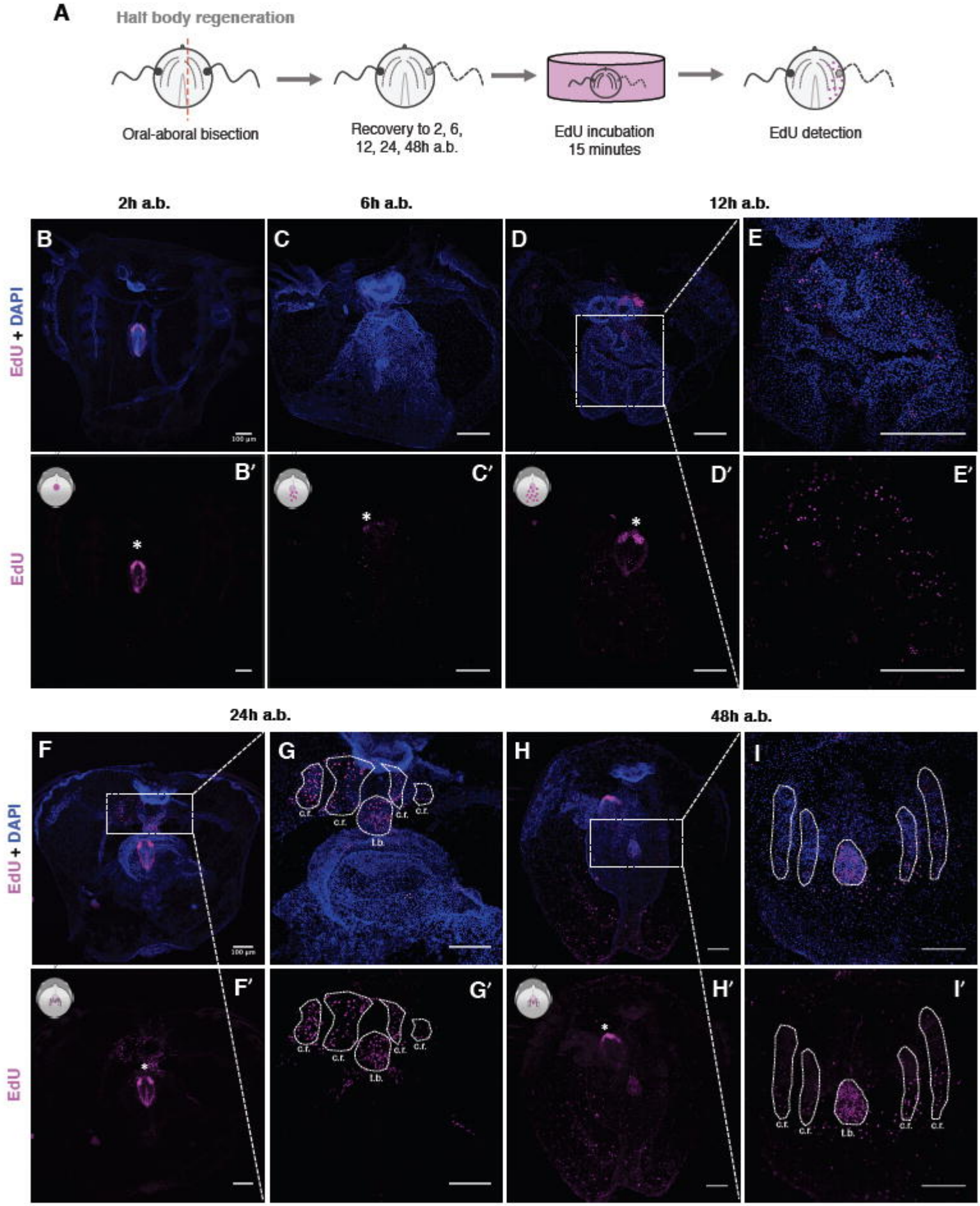
A
Half body regeneration
Oral-aboral bisection
Recovery to 2, 6, 12, 24, 48h a.b.
EdU incubation 15 minutes
EdU detection
2h a.b.
6h a.b.
12h a.b.
24h a.b.
48h a.b.
EdU + DAPI
EdU
B
C
D
E
B′
C′
D′
E′
F
G
H
I
F′
G′
H′
I′
100 µm
c.f.
l.b.

Figure 6

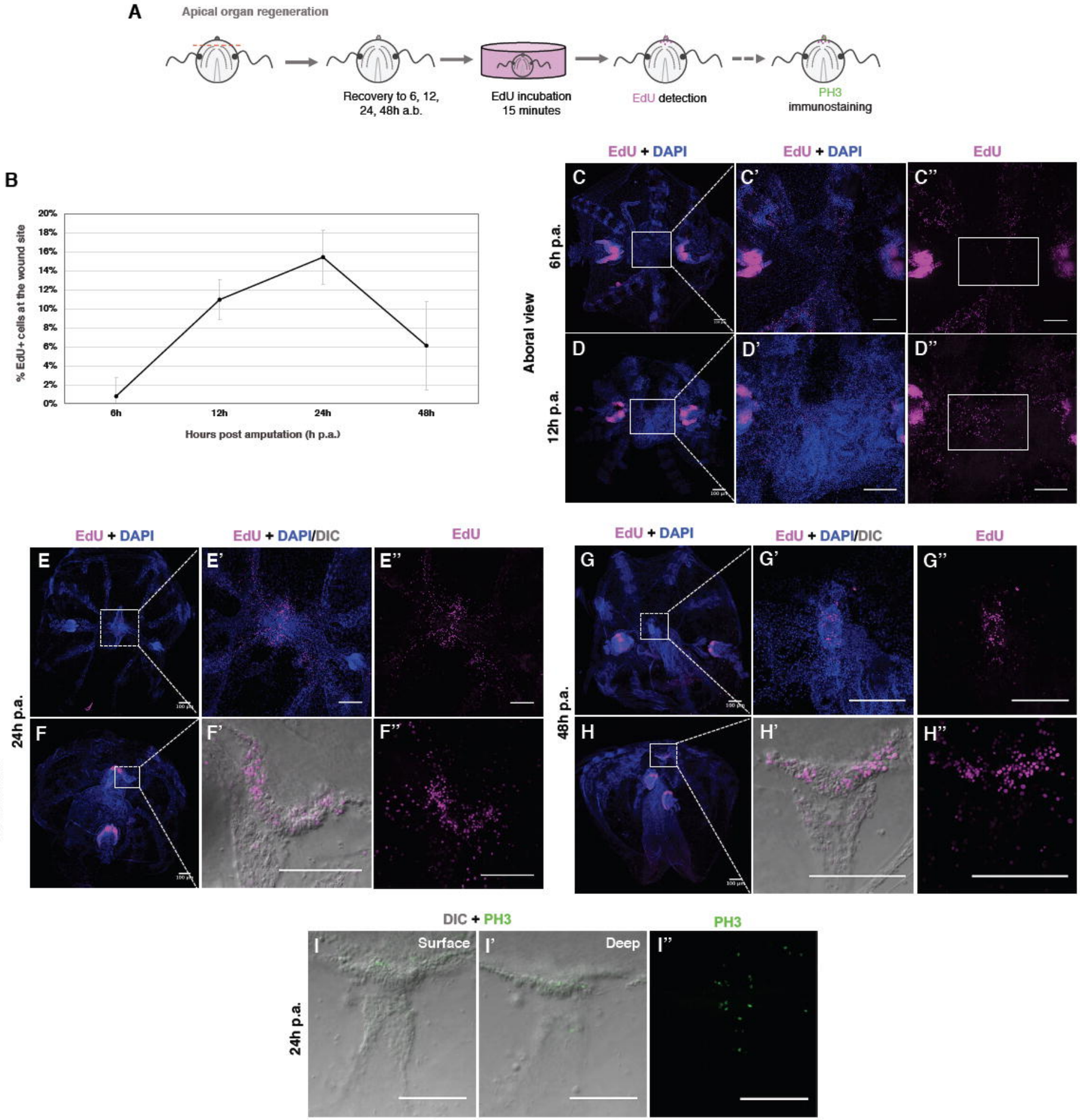
A
Apical organ regeneration
Recovery to 6, 12, 24, 48h a.b.
EdU incubation 15 minutes
EdU detection
PH3 immunostaining
B
% EdU+ cells at the wound site
20%
18%
16%
14%
12%
10%
8%
6%
4%
2%
0%
6h
12h
24h
48h
Hours post amputation (h p.a.)
EdU + DAPI
EdU + DAPI
EdU
Aboral view
6h p.a.
12h p.a.
C
C'
C''
D
D'
D''
EdU + DAPI
EdU + DAPI/DIC
EdU
Aboral view
Lateral view
24h p.a.
E
E'
E''
F
F'
F''
EdU + DAPI
EdU + DAPI/DIC
EdU
48h p.a.
G
G'
G''
H
H'
H''
DIC + PH3
PH3
24h p.a.
I
Surface
I'
Deep
I''

Figure 7

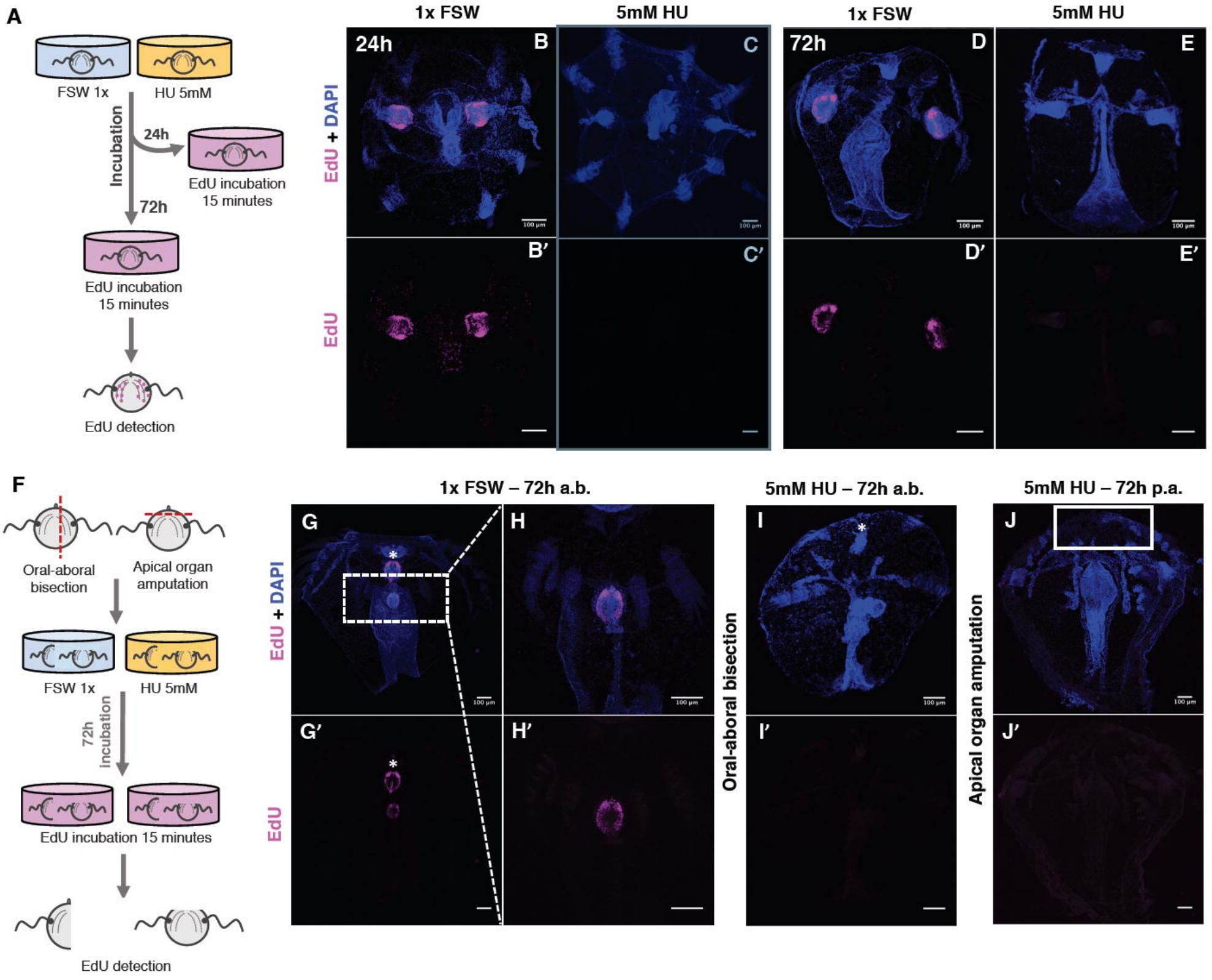
A
FSW 1x
HU 5mM
Incubation
24h
EdU incubation
15 minutes
72h
EdU incubation
15 minutes
EdU detection
1x FSW
5mM HU
1x FSW
5mM HU
24h
72h
B
C
D
E
B′
C′
D′
E′
EdU + DAPI
EdU
F
Oral-aboral
bisection
Apical organ
amputation
FSW 1x
HU 5mM
72h
incubation
EdU incubation 15 minutes
EdU detection
1x FSW – 72h a.b.
5mM HU – 72h a.b.
5mM HU – 72h p.a.
G
H
I
J
G′
H′
I′
J′
Oral-aboral bisection
Apical organ amputation
EdU + DAPI
EdU

Figure 8

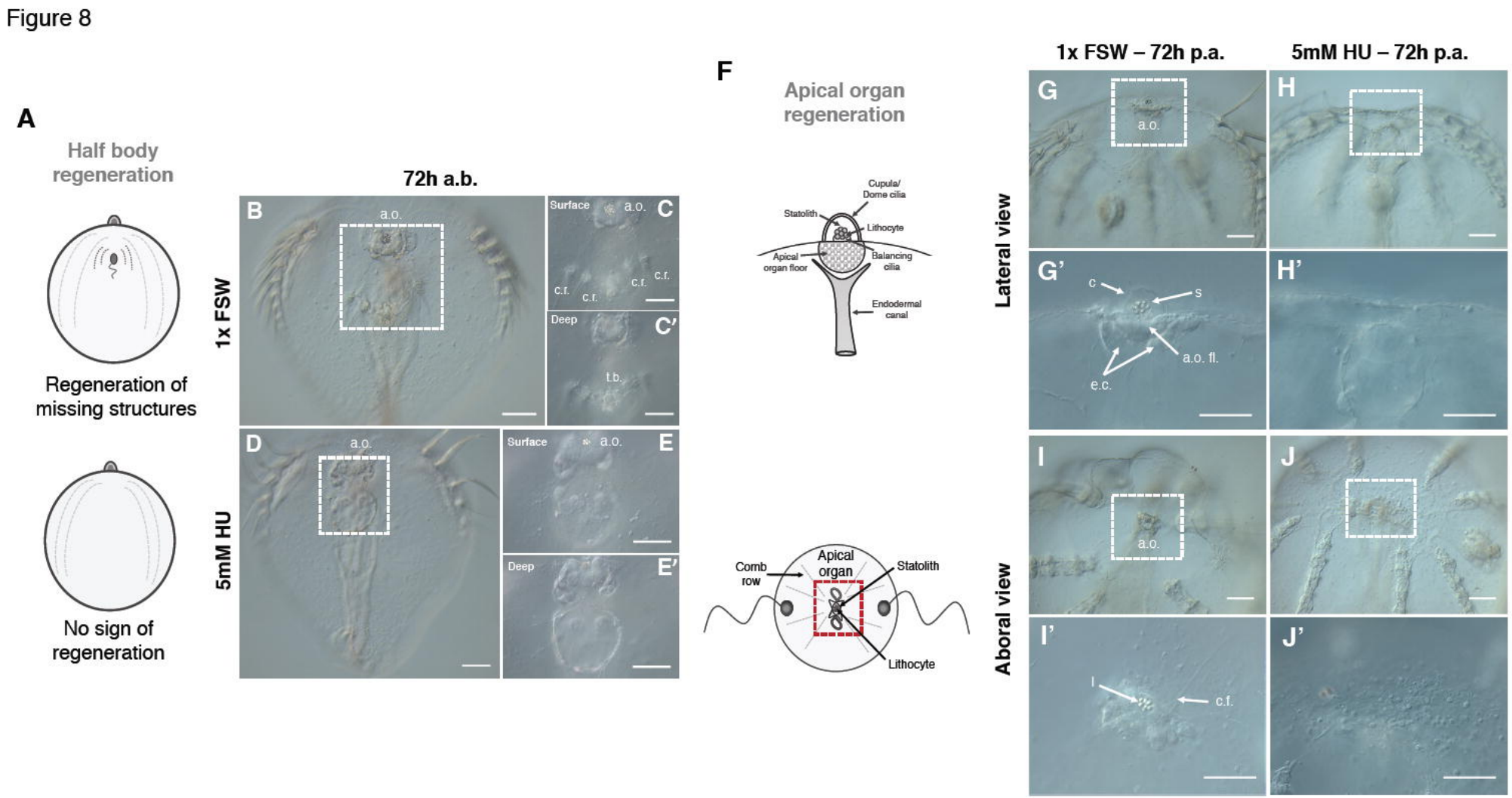
A
Half body regeneration
Regeneration of missing structures
No sign of regeneration
72h a.b.
1x FSW
5mM HU
B
a.o.
Surface
C
c.r.
Deep
C'
t.b.
D
E
E'
F
Apical organ regeneration
Cupula/ Dome cilia
Statolith
Lithocyte
Apical organ floor
Balancing cilia
Endodermal canal
Comb row
Apical organ
Statolith
Lithocyte
1x FSW – 72h p.a.
5mM HU – 72h p.a.
Lateral view
Aboral view
G
H
G'
H'
c
s
a.o. fl.
e.c.
I
J
I'
J'
l
c.f.

Figure 9

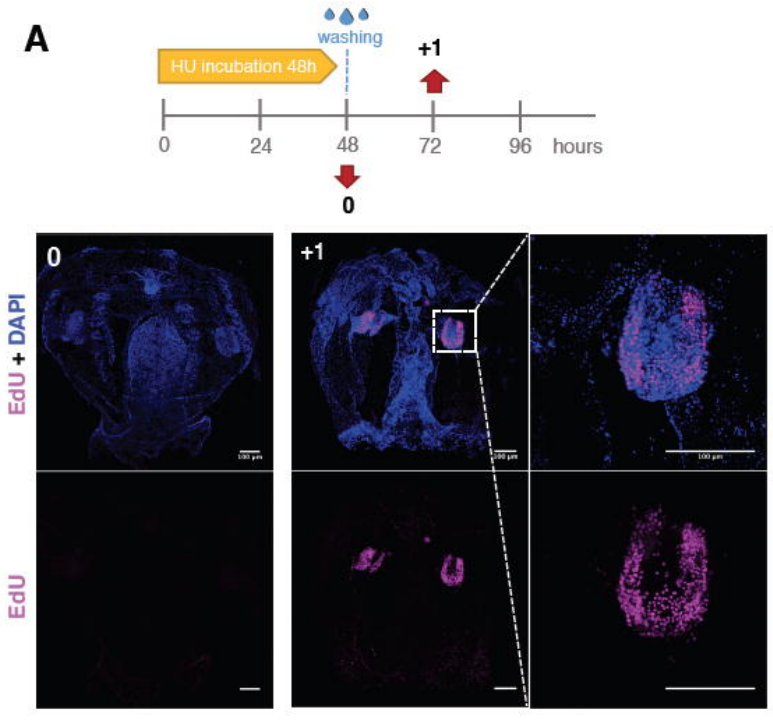
A
washing
HU incubation 48h
+1
0
24
48
72
96
hours
0
+1
EdU + DAPI
EdU

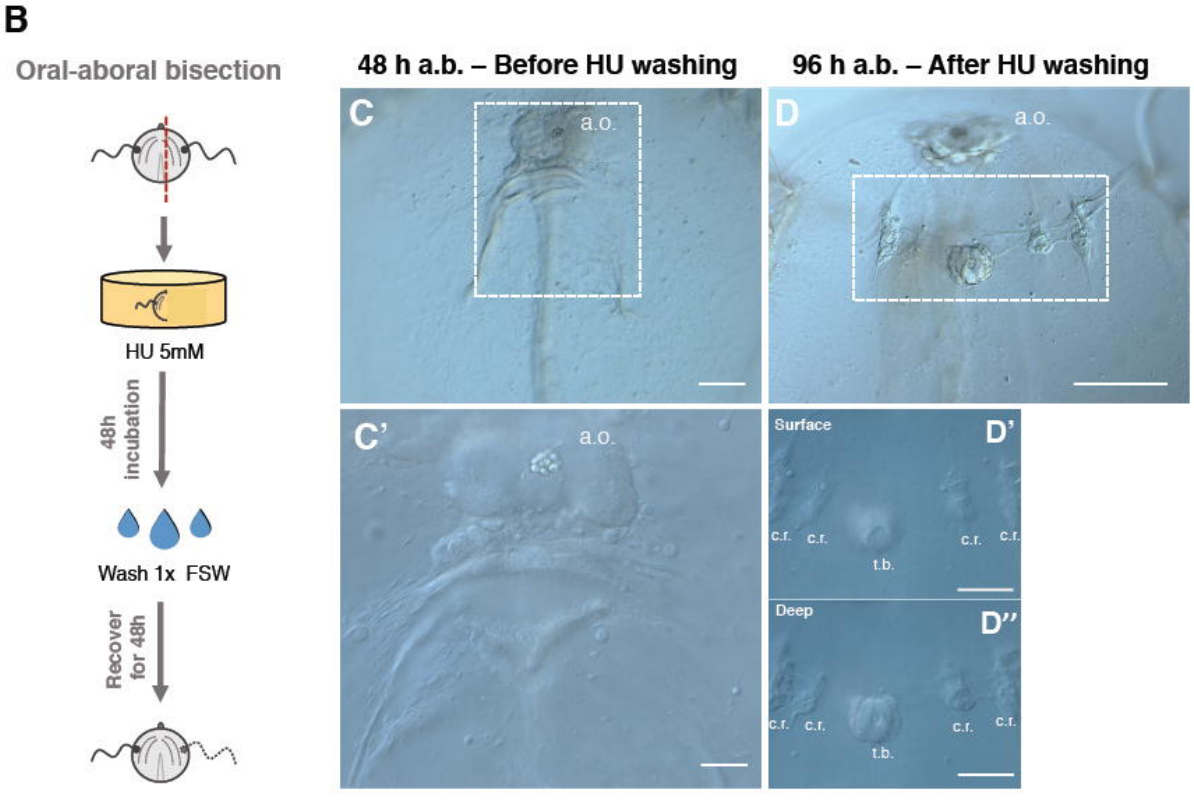
B
Oral-aboral bisection
HU 5mM
48h incubation
Wash 1x FSW
Recover for 48h
48 h a.b. – Before HU washing
96 h a.b. – After HU washing
C
a.o.
D
a.o.
C'
a.o.
Surface
D'
c.r.
t.b.
Deep
D''

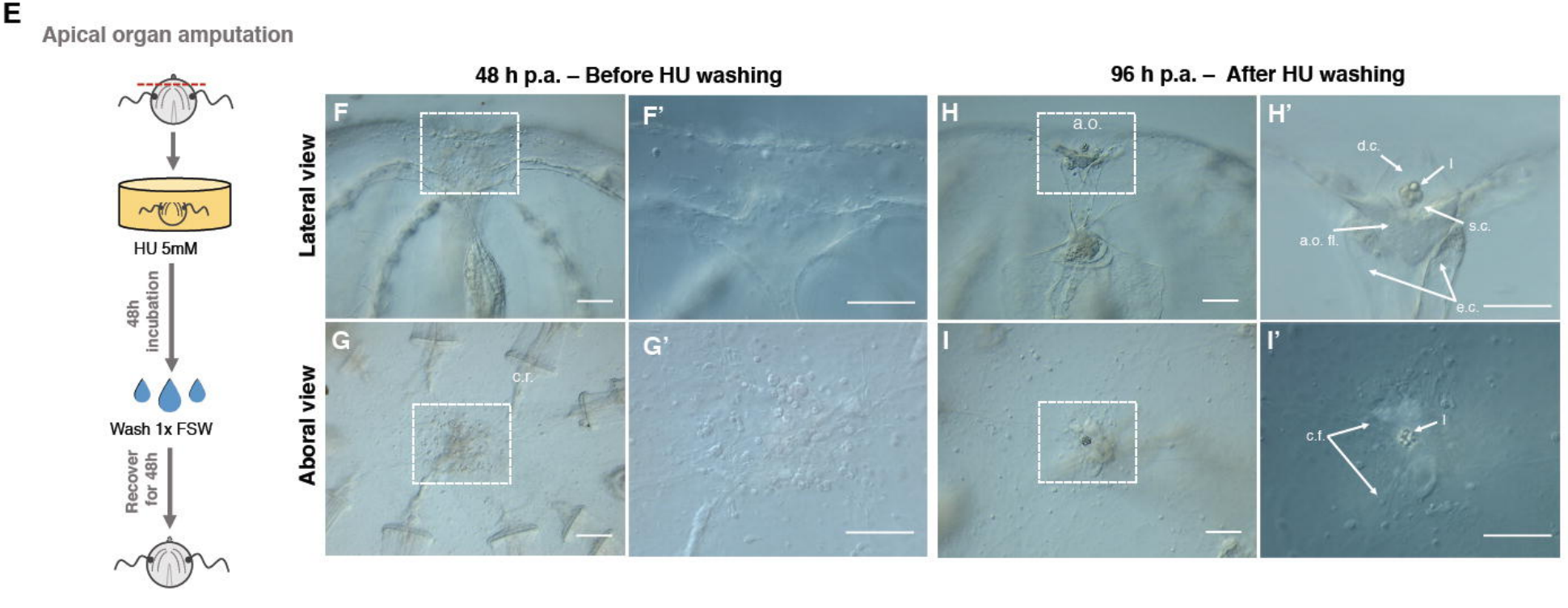
E
Apical organ amputation
HU 5mM
48h incubation
Wash 1x FSW
Recover for 48h
48 h p.a. – Before HU washing
96 h p.a. – After HU washing
Lateral view
Aboral view
F
F'
H
a.o.
H'
d.c.
l
s.c.
a.o. fl.
e.c.
G
c.r.
G'
I
I'
c.f.

Figure 10

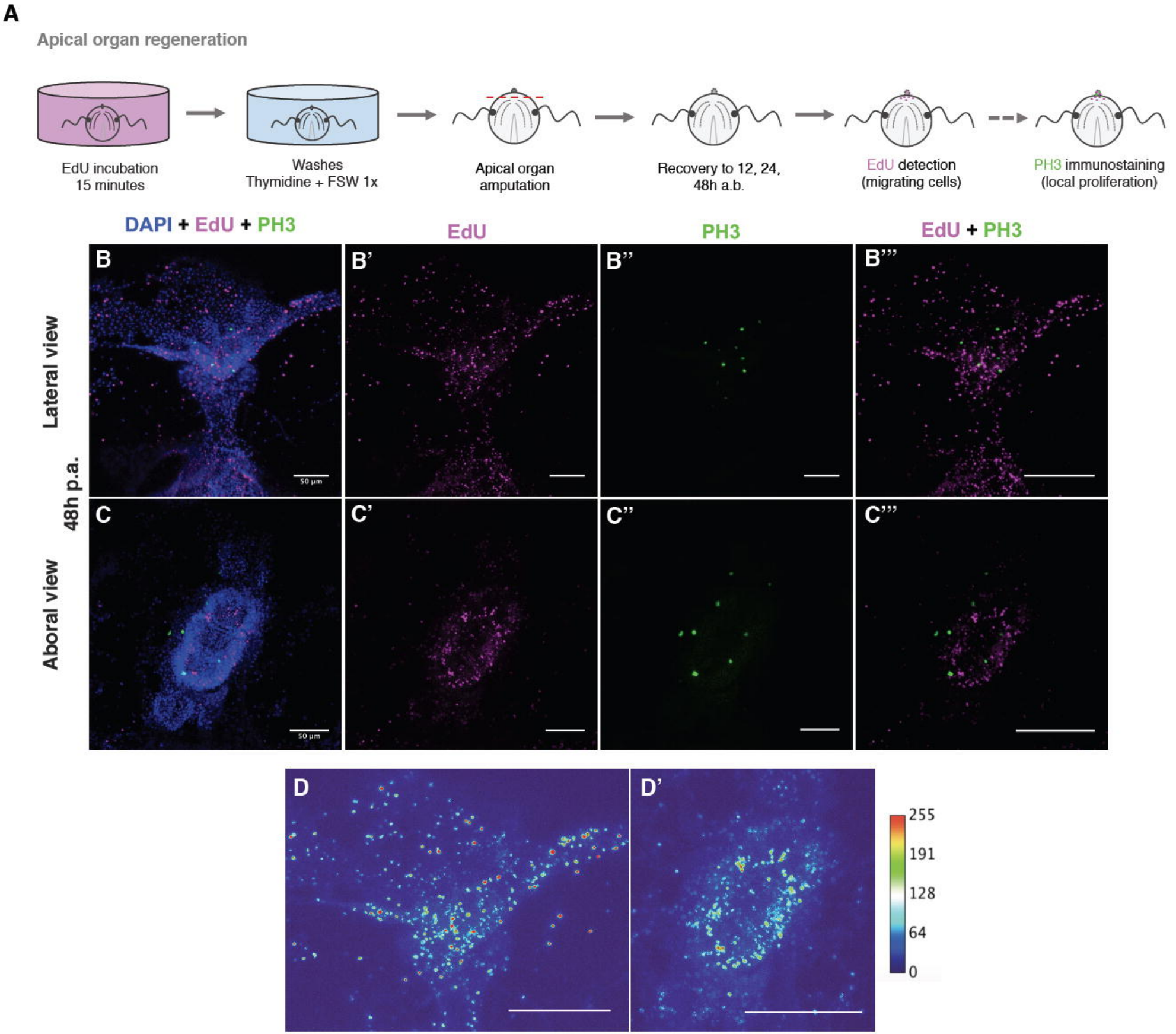
A
Apical organ regeneration
EdU incubation
15 minutes
Washes
Thymidine + FSW 1x
Apical organ
amputation
Recovery to 12, 24,
48h a.b.
EdU detection
(migrating cells)
PH3 immunostaining
(local proliferation)
DAPI + EdU + PH3
EdU
PH3
EdU + PH3
Lateral view
48h p.a.
Aboral view
B
B'
B''
B'''
C
C'
C''
C'''
50 µm
D
D'
255
191
128
64
0